520/1-83-019

PB84-106475

Analysis of Ocean Current Meter Records Obtained from a 1975 Deployment off the Farallon Islands, California

Battelle Pacific Northwest Labs., Richland, WA

Prepared for

Office of Radiation Programs, Washington, DC

Aug 83

TECHNICAL REPORT DATA
(Please read Instructions on the reverse before completing)

1. REPORT NO. EPA 520/1-83-019	2.	3. RECIPIENT'S ACCESSION NO. PB84 106475
4. TITLE AND SUBTITLE Analysis of Ocean Current Meter Records Obtained from a 1975 Deployment Off the Farallon Islands, California		5. REPORT DATE August 1983
		6. PERFORMING ORGANIZATION CODE
7. AUTHOR(S) David E. Crabbs		8. PERFORMING ORGANIZATION REPORT NO.
9. PERFORMING ORGANIZATION NAME AND ADDRESS Interstate Electronics Corporation Anaheim, California 92803		10. PROGRAM ELEMENT NO.
		11. CONTRACT/GRANT NO. IAG No. AD-89-F-1-607-0 Subcontract No. B-C2076-A-X
12. SPONSORING AGENCY NAME AND ADDRESS Office of Radiation Programs U.S. Environmental Protection Agency 401 M Street., S.W. Washington, D.C. 20460		13. TYPE OF REPORT AND PERIOD COVERED Final
		14. SPONSORING AGENCY CODE ANR-461
15. SUPPLEMENTARY NOTES		

16. ABSTRACT

Two bottom current records were obtained during August and September 1975 in the Farallon Islands low-level radioactive waste disposal area off San Francisco, California. This report presents the results of the data reduction and analysis of the curent meter records,and interprets the results with respect to additional data collected in 1977. An effort is made to compare the patterns of current activity in the dumpsite area for the time periods measured. It is proposed that while the possibility of transport of suspended material from within the dumpsite area cannot be ignored, conditions which prevailed at the time and location of measurements suggest that there is little tendency for shoreward transport of resuspended sediment. However, measurements taken throughout the year and over a wider area would be helpful in verifying this propositon.

17. KEY WORDS AND DOCUMENT ANALYSIS

a. DESCRIPTORS	b. IDENTIFIERS/OPEN ENDED TERMS	c. COSATI Field/Group
Ocean Dumping Ocean Disposal/Sea Disposal Low-Level Radioactive Waste Disposal Ocean Bottom Currents off California Radioactivity Transport		

18. DISTRIBUTION STATEMENT Unlimited Release	19. SECURITY CLASS (This Report) Unclassified	21. NO. OF PAGES 67
	20. SECURITY CLASS (This page) Unclassified	22. PRICE

EPA Form 2220-1 (Rev. 4-77) PREVIOUS EDITION IS OBSOLETE

United States
Environmental Protection
Agency

Office of
Radiation Programs
Washington DC 20460

EPA 520/1-83-019
August 1983

PB84-106475

Radiation

EPA

20

Analysis of Ocean Current Meter Records Obtained from a 1975 Deployment off the Farallon Islands, California

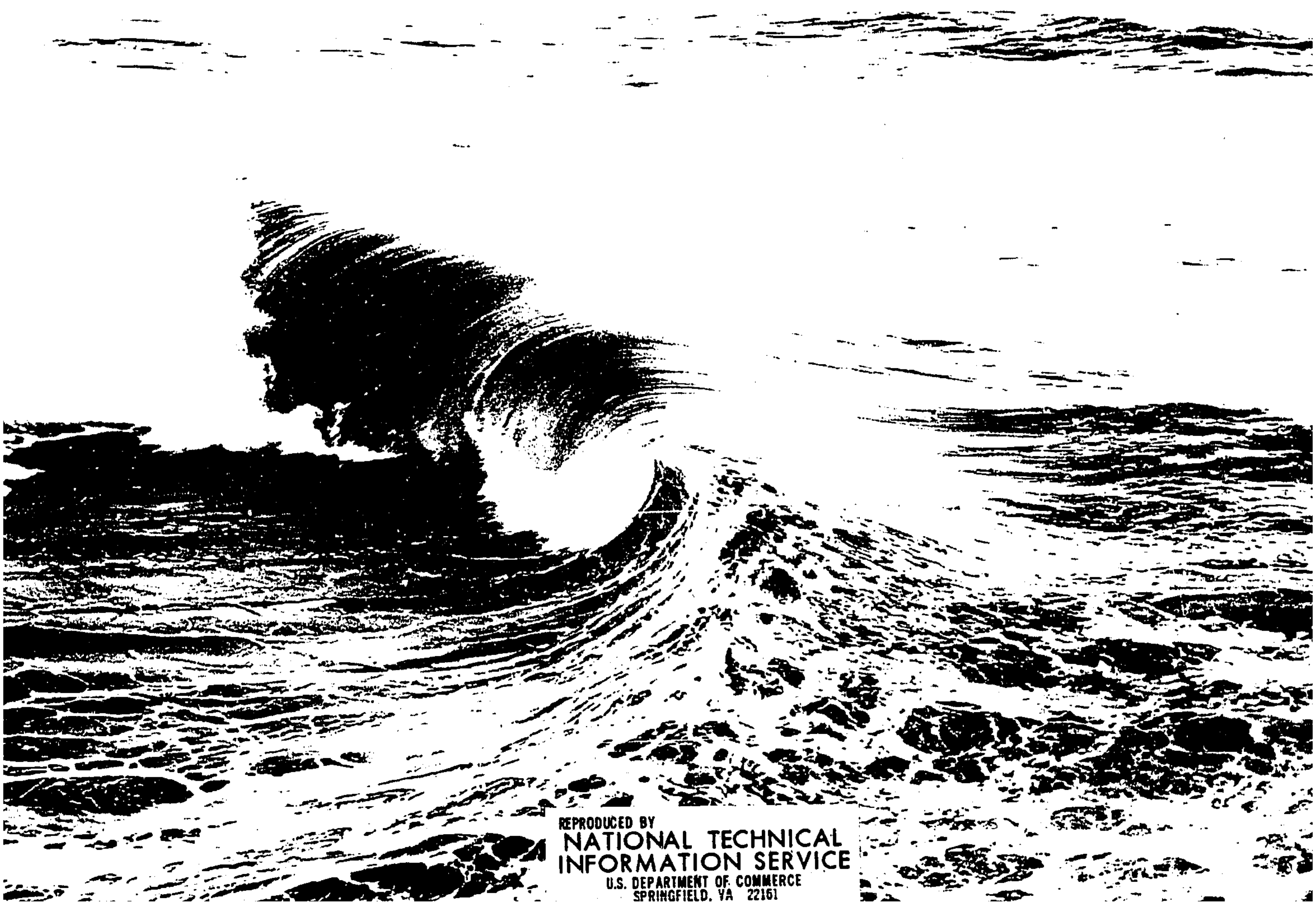

EPA REVIEW NOTICE

EPA 520/1-83-019

ANALYSIS OF OCEAN CURRENT METER RECORDS OBTAINED FROM A 1975 DEPLOYMENT OFF THE FARALLON ISLANDS, CALIFORNIA

By

David E. Crabbs

Interstate Electronics Corporation
Anaheim, California 92803

August 1983

This report was prepared as an account of contract work sponsored by the United States Environmental Protection Agency under Interagency Agreement No. AD-89-F-1-607-0 with Battelle Pacific Northwest Laboratories

Project Officer

Robert S. Dyer

Office of Radiation Programs
U.S. Environmental Protection Agency
Washington, DC 20460

FOREWORD

In response to the mandate of Public Law 92-532, the Marine Protection, Research, and Sanctuaries Act of 1972, as amended, the Environmental Protection Agency (EPA) has developed a program to promulgate regulations and criteria to control the ocean disposal of radioactive wastes. As part of that program, the EPA Office of Radiation Programs initiated feasibility studies in 1974 to learn whether present technologies could be used to determine the fate of radioactive wastes dumped in the past.

After successfully locating radioactive waste drums in previously used United States dumpsites, the Office of Radiation Programs developed a program of dumpsite-specific studies to look at the biological, chemical, and physical characteristics of the sites, and the presence and distribution of radionuclides within these sites.

A primary mechanism for physically dispersing and redistributing both soluble and particulate radioactive materials from a dumpsite is the action of ocean bottom currents. Of particular interest is the magnitude and direction of these currents. The present report discusses the results of two sets of ocean bottom current measurements obtained from the Farallon Islands 1700-meter low-level radioactive waste dumpsite area off California. These data are then compared with additional information collected two years later by EPA in an area east and slightly south of the 1700-meter dumpsite. The report concludes with a discussion of the velocity of the currents over the time period and area measured relative to large-scale currents off the California coast; and the possibility of shoreward transport of materials is examined.

The Agency invites all readers of this report to send any comments or suggestions to Mr. David E. Janes, Director, Analysis and Support Division, Office of Radiation Programs (ANR-461), Environmental Protection Agency, Washington, D.C. 20460.

Glen L. Sjoblom

Glen L. Sjoblom, Director
Office of Radiation Programs

ABSTRACT

This report addresses the reduction, analysis and interpretation of ocean current meter data records obtained during August and September 1975 in the vicinity of the radioactive waste disposal area near the Farallon Islands, off San Francisco, California. The data are interpreted in light of results from a later study which involved data taken in the same vicinity in the fall and winter months of 1977, and an effort is made to compare the two measurement programs and draw inferences about the patterns of current activity for the portions of the year for which satisfactory measurements were taken (i.e., late summer and autumn). It is proposed that while the possibility of transport of suspended material from within the dumpsite area cannot be ignored, for the locations and time periods measured, conditions which prevailed at the time of measurement in this report suggest that there is little tendency for shoreward transport of resuspended sediment. Measurements taken throughout the year and over a larger range, particularly closer to shore, would be helpful in verifying this proposition.

TABLE OF CONTENTS

Preceding page blank

LIST OF FIGURES

LIST OF TABLES

SECTION 1

INTRODUCTION

This report has been produced by Interstate Electronics Corporation for Battelle Pacific Northwest Laboratories of the Department of Energy in fulfillment of Subcontract Number B-C2076-A-X. The prime contract is between the U.S. Environmental Protection Agency, Office of Radiation Programs, and the Department of Energy and is being carried out under Interagency Agreement Number AD-89-F-607-0 by Battelle. The subject of this report consists of the reduction, analysis, and interpretation of ocean current meter data records obtained during August and September 1975 in the vicinity of the radioactive waste disposal area near the Farallon Islands. Also included is a discussion of the relationships between the 1975 measurements and the measurements taken in the same vicinity in late 1977 and early 1978. The latter measurements have been reported on by Interstate Electronics Corporation in "Farallon Islands Oceanographic Data Analysis," Volumes I and II, prepared under EPA Contract Number 68-01-0796, Modification Number 20, in May 1982. The intent of the present report is to analyze and interpret the 1975 data in the context of how it relates to the 1977-1978 measurement program, including the potential for suspended particle transport away from the dumpsite.

The remainder of this report includes six sections, numbered 2 to 7. Section 2 provides a summary of the work performed under this subcontract. Section 3 describes the meter array deployment and includes information relating to the 1977-1978 deployment program. Section 4 addresses the reduction and analysis of the 1975 data record, Section 5 offers interpretive results in the contexts mentioned above, and Section 6 presents results and conclusions. Pertinent references are listed in Section 7.

SECTION 2

SUMMARY

Four current meters were emplaced near the Farallon Islands low-level radioactive waste dumpsite, in August 1975, by the Scripps Institution of Oceanography of the University of California, San Diego. This study was undertaken to assess the current regime present in the dumpsite. Figure 2.1 shows the spatial relationship between the current meter locations, the dumpsite, the Farallon Islands, and the California coastline off San Francisco. The meter recovery operation took place approximately one month later and yielded two usable data records. These records were for two meters located at 37°37'30"N, 123°18'0"W and 37°38'30"N, 123°18'0"W at depths of 1729 m and 1849 m, respectively, and spaced approximately 2.3 km (1.3 nautical miles) apart. One of the records did not contain any directional information due to a hardware fault in the recording device, but the other record was subsequently analyzed by Dr. Richard Schwartzlose of Scripps. The analyses performed by Dr. Schwartzlose (Ref. 7) included generation of calibrated time history records, and the extraction of tidal currents for production of tidal ellipses and a progressive vector diagram. His results are referenced and briefly summarized in References 2 and 6.

The purpose of the present study is to extend the analyses performed by Dr. Schwartzlose on the 1975 data and to relate the results of this measurement program with a subsequent current measurement program performed in the same vicinity in 1977 and 1978.

The 1977-1978 current measurements were taken beginning in October 1977 using several Aanderaa current meters and a Vector Averaging Current Meter (VACM). The deployment period lasted for one year, and the results of five current meter records were reported on by Interstate Electronics Corporation (Reference 4).

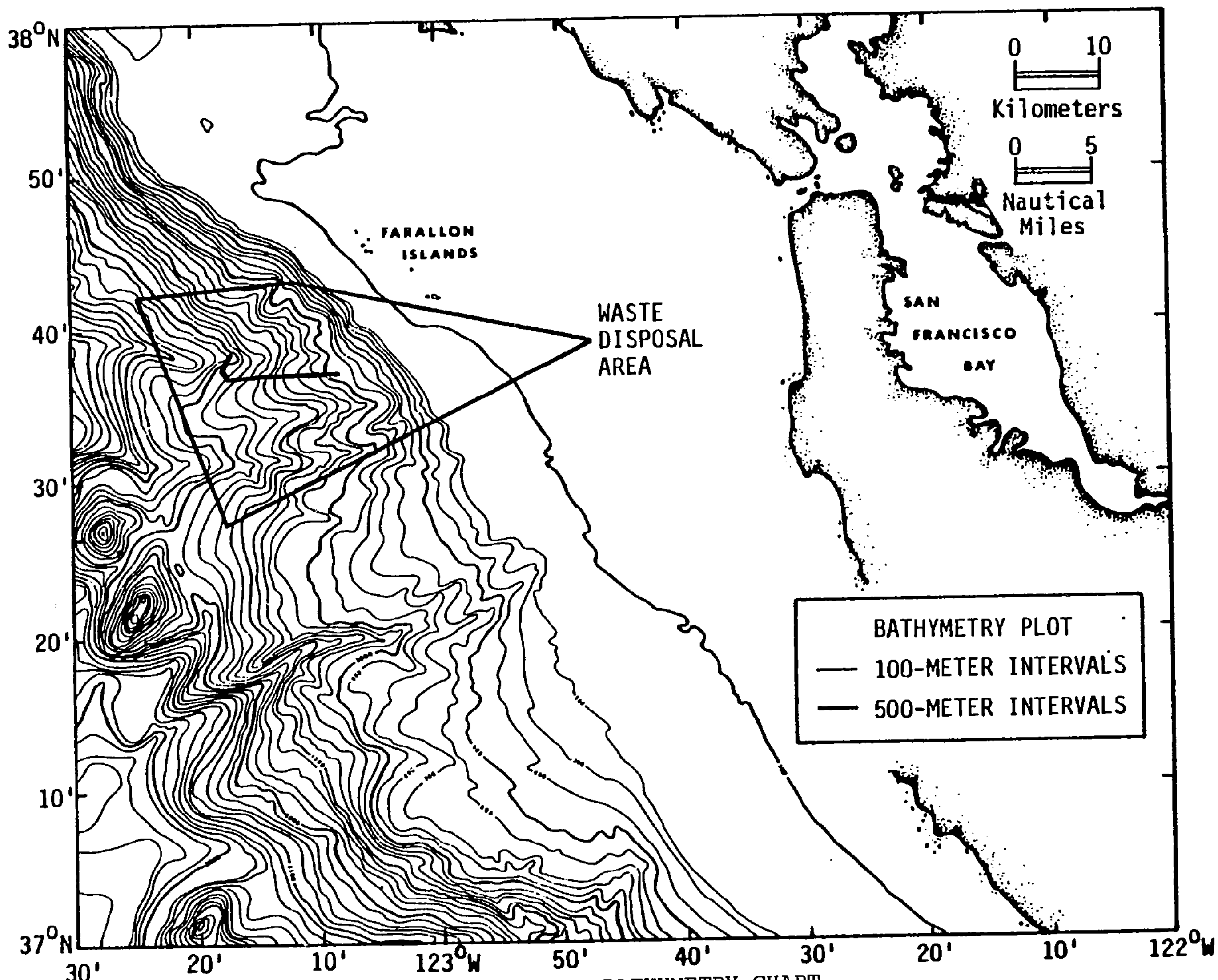

FIGURE 2.1: LOCAL BATHYMETRY CHART
SHOWING METER ARRAYS AND WASTE DISPOSAL AREA
(ADAPTED FROM REFERENCE 8)

The present study provides low-order statistical analysis of the 1975 data records, including summaries of the statistical moments, graphical representation of the time histories of the measured and derived parameters, histograms, and scatter diagrams. Further analysis includes the derivation of filtered time series of the orthogonal speed components, with tidal contributions removed, and the production of a progressive vector diagram and stick plot for the vector data. Power spectral density plots are also provided to allow resolution of the relative energy distribution among periodic current processes (i.e., tides, internal waves, inertial effects, etc.). The spectral analysis includes an assessment of the coherence of the different parameters at the frequencies associated with the major sources of periodic motion. Finally, the data from the 1975 measurement program are compared with the data from the 1977-1978 program, and an attempt is made to integrate the results into a broader characterization of ocean current activity in the vicinity of the Farallon Islands low-level radioactive waste dumpsite area. The results and conclusions from this effort are summarized in Section 6.

SECTION 3

METER DEPLOYMENT

This section concerns the deployment of the meters during the 1975 survey, and gives the operational scenario.

3.1 Description of Deployment

In August 1975, four Savonius-rotor current meters were deployed near the 1700 m Farallon Islands nuclear waste dumpsite. The meters were arranged in a rectangle, with one meter deployed approximately 2 m off the bottom at each corner. The distance between corners was approximately 1.6 kilometers and the center was located near the intersection of the 37°38'N parallel and 123°18'W meridian.

The meters, developed at the Scripps Institution of Oceanography, measured current speed to a 0.5 cm/sec sensitivity, and obtained directional measurements by means of a potentiometric compass. A strip chart recording medium was used, with the direction measurement indicated as a function of time on a scale from 0° to 360° magnetic. The speed was recorded in terms of the number of revolutions of the rotor in a given time period. Specifically, a mark was placed on the edge of the strip chart for each 16 turns of the rotor. Thus, the speed was a function of the number of marks per unit length of strip chart.

Two of the measurement records were successfully recovered 27 days after deployment. One was found to have no record of the current direction, although the speed record appeared to be properly recorded throughout the 27-day period. However, no analysis was made at that time. The other recovered record was found to be complete, and was subsequently calibrated and analyzed to generate tidal ellipses and a progressive vector diagram.

The reported locations, depths and times of operation for the two recovered meters are given in Table 3.1.

3.2 Array Location and Relation to 1977 Deployment

The reported locations, depths and times of operation for the five meters recovered from the 1977-1978 deployment period appear in Table 3.2. Note that only one of the five meters, the VACM, had data records covering the August-September period. However, as noted in the report on these meters (Reference 4), the recovered VACM time record was not preserved in its correct order, and reconstruction efforts were only partly successful. Nevertheless, some correspondence between the 1975 and 1977-1978 records should be observable by comparing the October/November time period in 1977 with the 1975 August/September record to see if a trend can be obtained. Published literature on surface currents and general phenomena in the Farallon Islands area can be used to judge the consistency of any observed trend with trends predicated by general knowledge of the area.

The locations of the five meters of the 1977-1978 program and the two meters deployed in 1975 (#1009 and #1028) are shown in Figure 3.1. Note that the distance units on the axes are in minutes of arc longitude, equivalent to 1 nautical mile (nm) on both axes. The 1977-1978 meters were emplaced approximately 0.8 kilometers south of the southern edge of the rectangle formed by the 1975 meters, and form an east/west line approximately 14.4 kilometers in length. Thus, the overall configuration of the seven meters from the two surveys is 'L' shape with 3 points defining an east/west reference and 3 points defining a north/south reference. The east/west portion of the 'L' is displaced in time from the remaining part by about 2 years and one month, and the central point on the north/south reference does not include directional information.

Figure 2.1 shows the configuration of the seven meters overlaid on a bathymetric chart of the Farallon Islands Waste Disposal Area. Reference 3 discusses the local bathymetry readings obtained during a 1974 survey conducted by IEC, while Reference 8 contains published bathymetry for the region.

TABLE 3.1

CURRENT METER DEPLOYMENTS-1975

METER NO.	START DATE/TIME	END DATE/TIME	NORTH LAT	WEST LONG	SITE DEPTH (m)	METER DEPTH (m)	COMMENTS
1009	8/21/75 21:00	9/17/75 15:30	37°37'30"	123°17'0"	1731	1729	NO DIRECTION RECORD
1028	8/22/75 2:30	9/17/75 17:00	37°38'30"	123°18'0"	1851	1849	

TABLE 3.2

CURRENT METER DEPLOYMENTS-1977

METER NO.	START DATE	END DATE	NORTH LAT	WEST LONG	SITE DEPTH (m)	METER DEPTH (m)	COMMENTS
2920	10/25/77	3/15/78	37°36'36"	123°07'32"	914	911	ARRAY B
2830	10/25/77	2/06/78	37°36'52"	123°14'46"	1372	912	ARRAY C. GAPS IN RECORD
VACM	10/25/77	10/24/78	37°36'52"	123°14'46"	1372	911	ARRAY C. TRANSPOSED TIME RECORDS
2918	10/25/77	12/21/77	37°36'51"	123°17'27"	1829	1800	ARRAY D
2919	10/25/77	3/10/78	37°36'51"	123°17'27"	1829	1826	ARRAY D

FIGURE 3.1: METER ARRAY LOCATIONS FOR 1975 AND 1977 DEPLOYMENTS

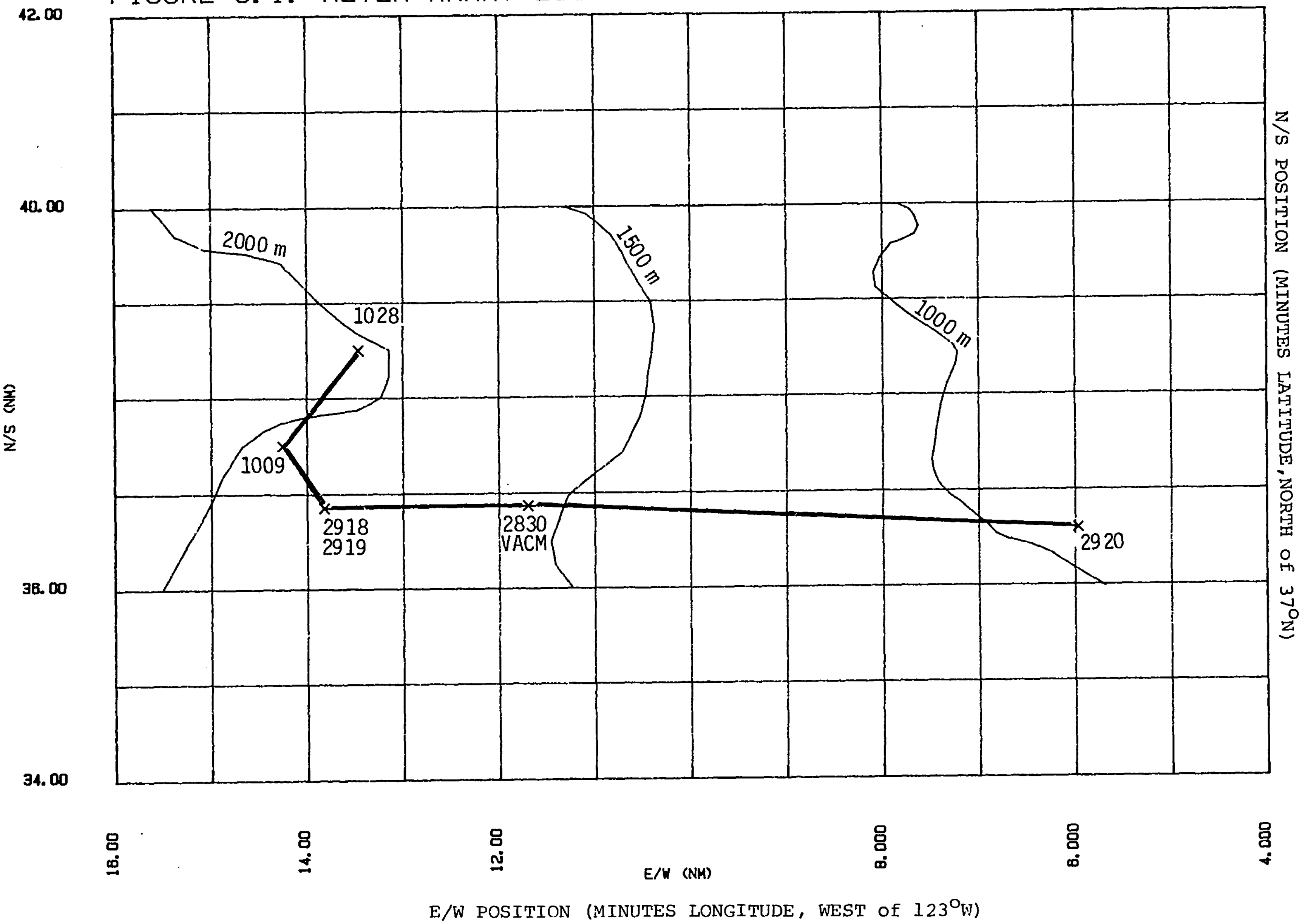

Figure 2.1 is largely adapted from Reference 8 with minor local adjustments resulting from data obtained in the 1974 survey. The meters cover an east/west transect close to the edge of the continental shelf.

SECTION 4

DATA REDUCTION AND ANALYSIS

The topics covered in this section include all of the data reduction and analysis performed on the two current meter records recovered in 1975. Comparisons with the 1977-1978 data are noted where pertinent.

4.1 Data Calibration

The two meter records recovered from the 1975 deployment required the speed record to be calibrated and converted to metric units of measure. The speed was recorded on a strip chart in terms of revolutions of the Savonius rotor. A mark was made on the strip chart each time the rotor completed 16 revolutions. Determining the velocity was thus a matter of counting the marks per unit length, and then scaling and calibrating the result to give centimeters per second. The scale factor used (i.e., 16) was multiplied by the number of marks per inch at each half hour interval (1 inch = 1 hour), and the result was calibrated by means of calibration curves provided by Scripps for the meters in question.

The direction record for meter number 1028 was read from the strip chart in terms of magnetic north. The magnetic variation from true north was determined to be 14 degrees east at the deployment site, so 14 degrees was added to each direction measurement to give the desired result in terms of true north.

4.2 Statistical Moments

The statistical moments (mean, standard deviation, skewness and kurtosis), along with the minimum and maximum speeds are provided on a daily basis for the speed record from meter number 1009 in Table 4.1. The summary statistics for the full 27-day deployment period are also given at the bottom of the table. The same statistical information is given for the speed record from meter number 1028 in Table 4.2. Tables 4.3 and 4.4 give statistics for the east/west

TABLE 4.1

SUMMARY STATISTICS FOR SPEED

CURRENT METER DATA FROM 1975 SURVEY
DAILY MOMENTS FOR CURRENT METER #1009

DATE	MEAN	MIN	MAX	STD. DEV.	SKEWNESS	KURTOSIS
8/21/75	10.81	9.06	15.16	2.03	1.07	2.81
8/22/75	6.75	1.38	17.87	4.29	.91	2.86
8/23/75	5.49	.00	16.10	3.53	.86	3.18
8/24/75	4.24	.00	11.02	2.36	.72	3.26
8/25/75	3.51	.00	7.64	1.74	.28	2.58
8/26/75	3.52	.00	7.64	2.00	.41	2.53
8/27/75	3.66	.00	8.43	1.96	.51	2.80
8/28/75	3.84	.00	10.23	2.05	.62	3.73
8/29/75	4.18	.00	10.23	2.68	.65	2.51
8/30/75	5.64	.00	17.31	3.80	.84	3.20
8/31/75	4.11	1.38	10.23	2.29	1.04	3.15
9/01/75	5.18	.00	17.31	3.03	1.24	6.27
9/02/75	4.31	.00	11.58	2.78	.63	2.50
9/03/75	4.49	.00	13.98	2.82	.91	4.16
9/04/75	5.49	.00	16.75	4.56	.96	2.65
9/05/75	6.60	1.38	20.61	4.15	1.29	4.77
9/06/75	7.26	1.38	13.42	3.02	.04	2.38
9/07/75	4.61	.00	13.42	2.83	1.00	3.73
9/08/75	3.69	.00	6.92	2.04	.24	1.88
9/09/75	5.55	.00	19.87	4.49	1.60	4.90
9/10/75	7.48	1.38	18.44	4.12	.84	3.09
9/11/75	7.95	1.38	17.87	4.33	.15	1.89
9/12/75	8.12	.00	18.44	4.72	.20	2.19
9/13/75	8.03	1.38	17.31	3.89	.20	2.09
9/14/75	6.75	.00	12.85	2.92	-.11	2.24
9/15/75	5.05	1.38	11.58	2.70	.70	2.62
9/16/75	5.34	.00	11.58	3.09	.32	2.12
9/17/75	9.05	1.38	16.75	3.61	-.24	2.37

TOTAL PERIOD MOMENTS FOR CURRENT METER #1009

TOTAL DAYS	MEAN	MIN	MAX	STD. DEV.	SKEWNESS	KURTOSIS
27	5.54	.00	20.61	3.63	1.04	3.92

TABLE 4.2

SUMMARY STATISTICS FOR SPEED

CURRENT METER DATA FROM 1975 SURVEY
DAILY MOMENTS FOR CURRENT METER #1028

DATE	MEAN	MIN	MAX	STD. DEV.	SKEWNESS	KURTOSIS
8/22/75	3.82	.80	8.43	1.85	.42	2.48
8/23/75	4.67	.00	10.63	2.93	.39	1.94
8/24/75	4.15	1.38	11.02	2.27	1.14	3.99
8/25/75	4.15	.80	9.65	1.93	.43	2.82
8/26/75	3.69	.80	9.36	1.92	.88	3.21
8/27/75	3.28	.00	7.64	1.58	.61	3.10
8/28/75	4.04	.80	11.58	2.26	1.50	5.81
8/29/75	3.71	1.38	11.02	2.05	1.57	5.72
8/30/75	6.48	.80	13.13	3.67	.17	1.62
8/31/75	5.97	1.88	13.70	2.94	.53	2.20
9/01/75	5.87	.00	14.83	3.32	.92	3.52
9/02/75	6.38	.80	14.26	3.17	.26	2.23
9/03/75	6.62	1.38	18.15	3.83	.92	3.76
9/04/75	6.67	1.38	13.42	3.22	.27	2.01
9/05/75	6.80	1.88	16.47	3.40	.62	2.95
9/06/75	5.30	1.38	13.13	3.00	.99	3.41
9/07/75	5.34	1.38	12.10	2.41	.73	3.24
9/08/75	4.87	.80	11.02	2.52	.70	2.55
9/09/75	6.41	1.88	11.34	2.62	.06	1.98
9/10/75	5.76	.00	17.31	3.71	1.00	3.91
9/11/75	4.94	1.38	9.06	2.26	.13	1.75
9/12/75	5.46	1.88	12.85	2.81	.77	2.67
9/13/75	4.21	.80	9.06	2.40	.36	1.96
9/14/75	3.43	.80	9.36	1.83	.91	3.74
9/15/75	3.74	.00	10.63	2.22	1.28	4.31
9/16/75	8.17	1.88	14.55	3.29	-.20	2.27
9/17/75	8.95	3.11	16.75	3.41	.46	2.66

TOTAL PERIOD MOMENTS FOR CURRENT METER #1028

TOTAL DAYS	MEAN	MIN	MAX	STD. DEV.	SKEWNESS	KURTOSIS
26	5.26	.00	18.15	3.07	.93	3.62

TABLE 4.3

SUMMARY STATISTICS FOR E/W COMPONENT

CURRENT METER DATA FROM 1975 SURVEY
DAILY MOMENTS FOR CURRENT METER #1028

DATE	MEAN	MIN	MAX	STD.DEV.	SKEWNESS	KURTOSIS
8/22/75	.97	-5.40	6.22	2.92	-.40	2.40
8/23/75	1.33	-10.60	8.41	4.48	-.83	3.20
8/24/75	-.18	-9.88	10.96	3.92	.52	3.84
8/25/75	.57	-7.21	6.32	3.52	-.33	2.34
8/26/75	.23	-6.98	8.41	3.46	.08	2.60
8/27/75	.32	-7.34	4.23	2.72	-.87	3.03
8/28/75	.35	-7.34	4.90	3.14	-.75	2.63
8/29/75	-.17	-11.00	6.01	3.85	-.79	3.15
8/30/75	-.43	-12.62	9.91	6.55	-.27	1.89
8/31/75	-.10	-13.17	8.01	5.80	-.48	2.07
9/01/75	-.25	-13.33	8.41	6.16	-.45	2.20
9/02/75	-.27	-14.19	9.83	6.31	-.22	1.96
9/03/75	.12	-17.62	9.55	6.35	-.83	3.30
9/04/75	.31	-12.90	10.19	6.66	-.48	2.00
9/05/75	-.81	-16.38	9.55	7.02	-.44	1.88
9/06/75	.26	-11.80	7.21	4.99	-.99	3.09
9/07/75	.98	-10.20	10.87	4.62	-.06	2.40
9/08/75	-.06	-9.91	8.71	4.36	-.12	2.46
9/09/75	.50	-10.90	9.55	5.95	-.37	1.72
9/10/75	-.93	-16.64	7.33	5.70	-.83	3.30
9/11/75	-.13	-8.41	7.08	4.31	-.33	1.96
9/12/75	.15	-12.78	9.83	5.12	-.72	2.72
9/13/75	-.06	-6.99	6.65	3.57	-.05	2.45
9/14/75	.03	-6.32	7.57	2.84	.05	2.80
9/15/75	-1.21	-10.57	4.28	3.26	-1.00	3.88
9/16/75	1.10	-14.47	10.19	7.74	-.47	1.81
9/17/75	-.19	-16.66	10.13	8.55	-.41	1.77

TOTAL PERIOD MOMENTS FOR CURRENT METER #1028

TOTAL DAYS	MEAN	MIN	MAX	STD.DEV.	SKEWNESS	KURTOSIS
26	.09	-17.62	10.96	5.14	-.55	3.14

TABLE 4.4

SUMMARY STATISTICS FOR N/S COMPONENT

CURRENT METER DATA FROM 1975 SURVEY
DAILY MOMENTS FOR CURRENT METER #1028

DATE	MEAN	MIN	MAX	STD. DEV.	SKEWNESS	KURTOSIS
8/22/75	.64	-4.51	8.17	2.90	.76	2.81
8/23/75	1.85	-3.12	8.48	2.33	.52	3.08
8/24/75	1.34	-4.28	6.32	2.34	-.26	2.73
8/25/75	1.44	-6.94	6.65	2.54	-.75	4.44
8/26/75	1.32	-2.83	6.72	1.95	.04	3.15
8/27/75	1.48	-2.34	6.32	1.94	.39	2.91
8/28/75	1.02	-5.26	10.41	3.28	.49	3.43
8/29/75	1.09	-2.50	3.72	1.48	-.49	2.76
8/30/75	1.52	-4.97	9.24	3.31	.27	2.46
8/31/75	1.65	-4.97	8.00	2.94	-.07	2.58
9/01/75	.65	-6.50	4.95	2.79	-.75	2.89
9/02/75	1.01	-4.97	8.00	3.28	.05	2.18
9/03/75	2.14	-4.48	13.29	3.80	.73	3.33
9/04/75	1.91	-3.97	8.24	2.77	-.32	2.76
9/05/75	1.17	-5.50	6.48	2.73	-.49	2.52
9/06/75	.95	-6.80	7.71	3.44	-.50	2.55
9/07/75	1.18	-5.71	6.51	3.34	-.38	2.13
9/08/75	1.46	-4.95	8.92	3.06	-.06	2.86
9/09/75	1.81	-4.83	9.36	3.14	-.10	2.88
9/10/75	1.79	-4.77	8.38	3.32	-.19	2.26
9/11/75	.80	-4.95	6.38	3.29	-.09	1.78
9/12/75	.91	-5.18	7.99	3.36	-.06	2.25
9/13/75	1.33	-4.77	8.27	3.06	.24	2.30
9/14/75	1.55	-2.75	6.38	2.20	.25	2.61
9/15/75	1.10	-5.13	6.01	2.42	-.41	2.80
9/16/75	1.48	-6.65	7.36	3.94	-.28	1.80
9/17/75	1.27	-8.55	8.10	4.39	-.59	2.49

TOTAL PERIOD MOMENTS FOR CURRENT METER #1028

TOTAL DAYS	MEAN	MIN	MAX	STD. DEV.	SKEWNESS	KURTOSIS
26	1.33	-8.55	13.29	2.98	-.07	3.17

component and the north/south component, respectively, for meter number 1028. The components could not be resolved for meter number 1009 since it did not record direction.

Examination of the statistics for the speed record for the two meters shows them to be comparable, with their means differing from each other by only about 5%. Meter number 1009 had the higher mean, and was found to also have slightly higher moments and a slightly higher maximum. The distributions for both meters had positive skewnesses of around 1.0, and were both slightly more kurtotic than the normal distribution (which has a kurtosis of 3.0). Positive skewness indicates that the distributions tail off towards higher speeds, and the kurtosis indicates that the distributions are slightly peaked.

Table 4.5 gives statistics for the five meters deployed in 1977-1978 for the last week of October 1977 and month of November 1977 (the first full month of deployment). With the exception of meter number 2920 and the October portion of the record for 2918, all of the meters have somewhat greater mean speeds than those measured by 1009 and 1028. However, meter number 2920 was located in the shallowest part of the deployment site fairly close to the edge of the continental shelf, and was moored just off the bottom, measuring bottom currents at a depth of about 900 meters. The observed trends suggest a reduction in bottom current speed with progression up the continental shelf. Regarding the other four meters, numbers 2918 and 2919 measured deep bottom currents at around 1800 meters, and number 2830 and the VACM measured mid-water column currents at the 900 meter level in a 1400 meter depth location.

The component statistics for the five 1977-1978 meters are given for the last week of October and the month of November in Table 4.6. The component statistics for meter number 1028 are closest in character to those of meter number 2919. Both meters indicate a substantial mean northward flow, with some additional average flow eastward. Both are located near the deeper western edge of the dumpsite study area.

TABLE 4.5: SPEED MOMENTS

METER NO.	MEAN (cm/sec)	MINIMUM	MAXIMUM	STANDARD DEVIATION	SKEWNESS	KURTOSIS
2920-OCT	4.16	0.	14.	2.49	.93	4.40
2920-NOV	4.77	0.	28.	2.82	.76	3.90
2830-OCT	6.46	0.	20.	3.51	.36	3.38
2830-NOV	6.07	0.	18.	3.60	.34	2.84
VACM-OCT	6.18	2.	17.	2.81	.70	3.18
VACM-NOV	6.73	2.	21.	3.11	.57	2.95
2918-OCT	5.25	2.	15.	2.84	.55	2.80
2918-NOV	6.35	2.	25.	3.83	1.15	4.89
2919-OCT	5.74	0.	17.	2.94	.83	3.66
2919-NOV	6.58	0.	25.	3.71	1.12	4.91
1009-'75 (AUG/SEP)	5.54	0.	21.	3.63	1.04	3.92
1028-'75 (AUG/SEP)	5.26	0.	18.	3.07	.93	3.62

TABLE 4.6: COMPONENT MOMENTS

METER NO.		MEAN (cm/sec)	MINIMUM	MAXIMUM	STANDARD DEVIATION	SKEWNESS	KURTOSIS
2920-OCT	(E/W)	-.25	-12.	13.	3.81	-.02	3.89
2920-NOV		-.13	-19.	17.	4.21	-.04	3.37
2920-OCT	(N/S)	.48	-9.	10.	3.02	-.19	3.14
2920-NOV		.19	-12.	28.	3.56	.61	6.63
2830-OCT	(E/W)	-.55	-16.	12.	5.05	.19	2.52
2830-NOV		-.20	-13.	16.	4.65	.05	2.81
2830-OCT	(N/S)	.06	-19.	13.	5.31	-.15	3.03
2830-NOV		.52	-16.	15.	5.27	-.18	2.80
VACM-OCT	(E/W)	-.44	-12.	13.	4.94	.26	2.40
VACM-NOV		-.26	-14.	14.	5.01	.04	2.46
VACM-OCT	(N/S)	.56	-13.	16.	4.55	.11	2.80
VACM-NOV		.95	-19.	15.	5.33	-.18	2.58
2918-OCT	(E/W)	1.97	-9.	14.	4.81	.17	2.34
2918-NOV		1.42	-24.	22.	6.56	-.36	3.27
2918-OCT	(N/S)	.61	-7.	9.	2.88	.18	2.81
2918-NOV		.42	-13.	13.	3.14	-.17	4.25
2919-OCT	(E/W)	1.04	-11.	14.	4.80	.16	2.52
2919-NOV		.43	-23.	20.	6.20	-.41	3.64
2919-OCT	(N/S)	1.75	-11.	17.	3.81	.35	3.92
2919-NOV		1.77	-12.	16.	3.90	.15	3.60
1028 (AUG/SEP)	(E/W)	.09	-18.	11.	5.14	-.55	3.14
1028 (AUG/SEP)	(N/S)	1.33	-9.	13.	2.98	-.07	3.17

4.3 Histograms and Scatter Diagrams

Histograms are provided for the speed records for both meter 1009 (Figure 4.1) and meter 1028 (Figure 4.2). Both histograms have peaks in the 2 cm/sec to 3 cm/sec class interval, indicating that the most likely speed measurement for both meters is in this vicinity. The histograms both display the positive skewness predicted by the summary statistics.

Histograms for the east/west and north/south components for meter number 1028 are shown in Figures 4.3 and 4.4, respectively. The east/west component has virtually a zero mean, with a modal peak in the 0 cm/sec to 2 cm/sec range. The distribution is visibly skewed in the western direction (i.e., negatively). The north/south component, on the other hand, is not visibly skewed, but shows a northward mean current, again with a modal peak in the 0 cm/sec to 2 cm/sec region. The distribution is considerably more confined than the one for the east/west component, indicating that the flow is generally less variable in the north/south direction. This is also evidenced by the standard deviations for the two distributions.

Scatter diagrams have been generated relating the east/west and north/south speed components and the speed and direction for meter number 1028. The speed versus direction scatter diagram shows significant correlation and indicates that the greatest speeds occurred in conjunction with direction readings of about 250° to 270° true (Figure 4.5). However, a modal peak occurs at about 4 cm/sec and 45° true. Almost 25% of the observed direction records fell between 22.5° and 45° true. The scatter diagram for the speed components (Figure 4.6) also shows the extreme velocity events tailing off to the west and indicates a modal peak in the northeast quadrant. The relatively greater magnitude of variance along the east/west axis is readily apparent.

An additional scatter diagram (Figure 4.7) was calculated to compare the speed records for meters 1009 and 1028 with each other. The two records are not highly correlated, especially with regard to joint high velocity events. However, a modal peak exists in the region of 4 cm/sec for meter 1028 and 3 cm/sec for meter 1009.

FIGURE 4.1: HISTOGRAM OF SPEED (CM/SEC) FOR METER 1009

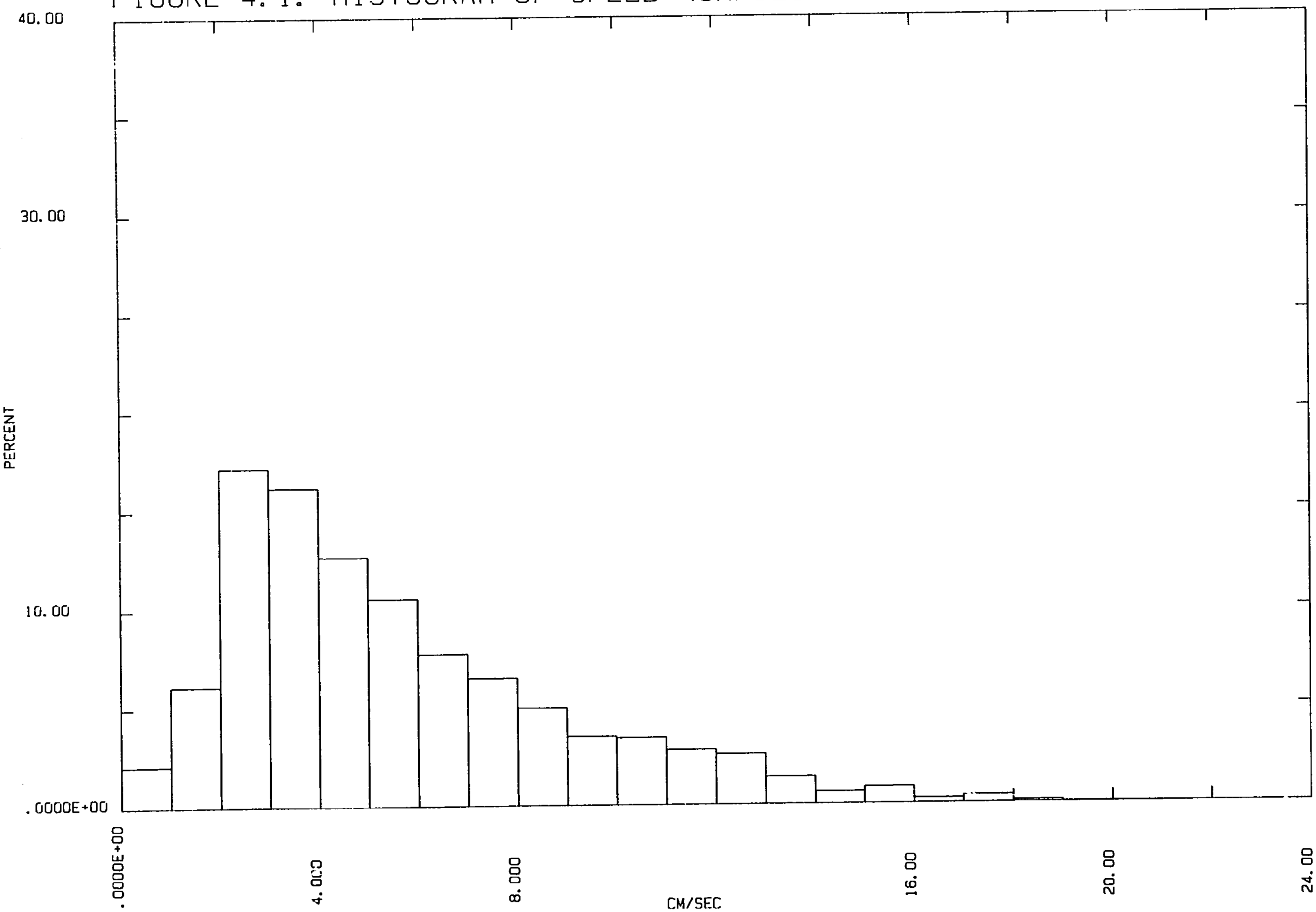

FIGURE 4.2: HISTOGRAM OF SPEED (CM/SEC) FOR METER 1028

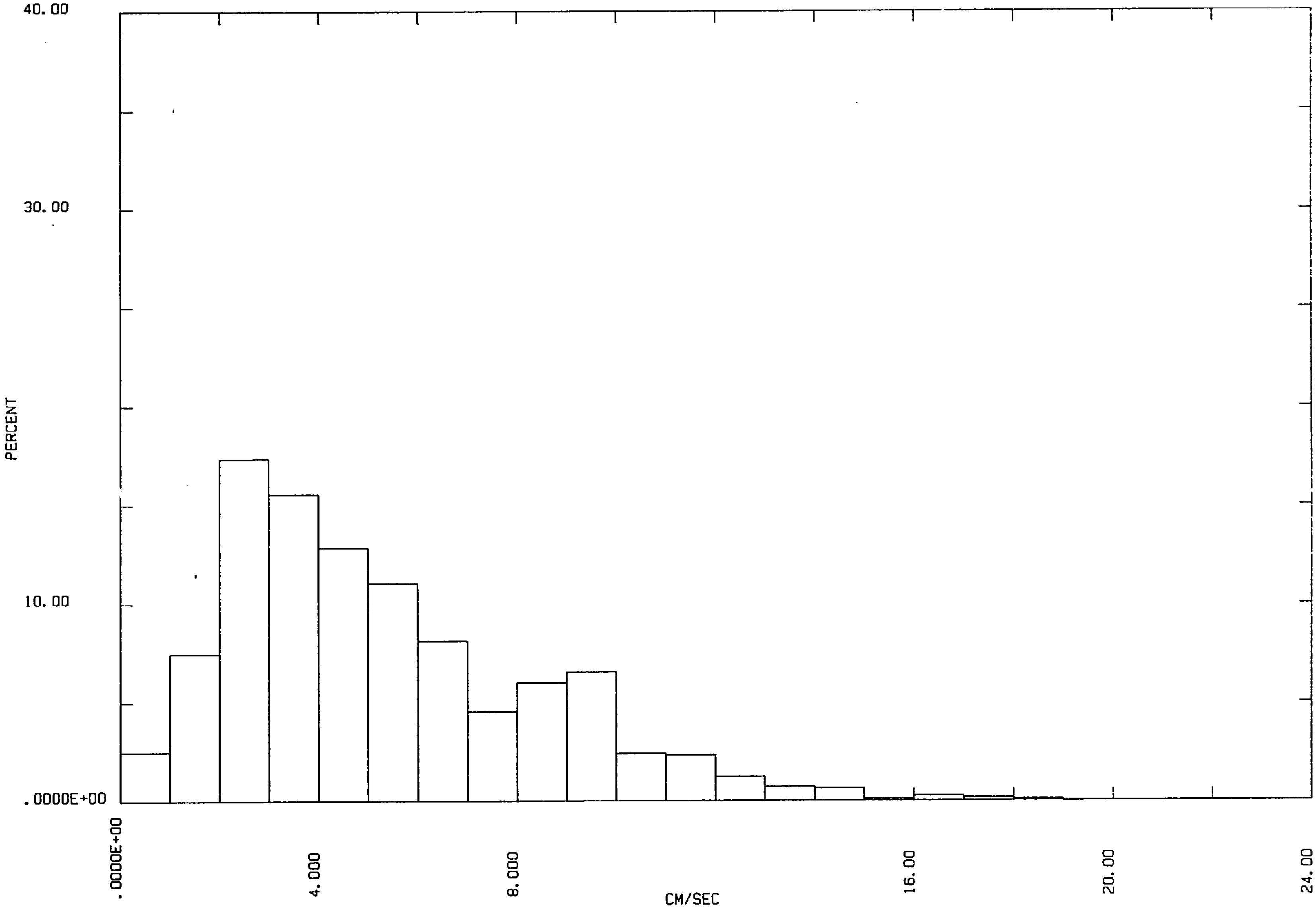

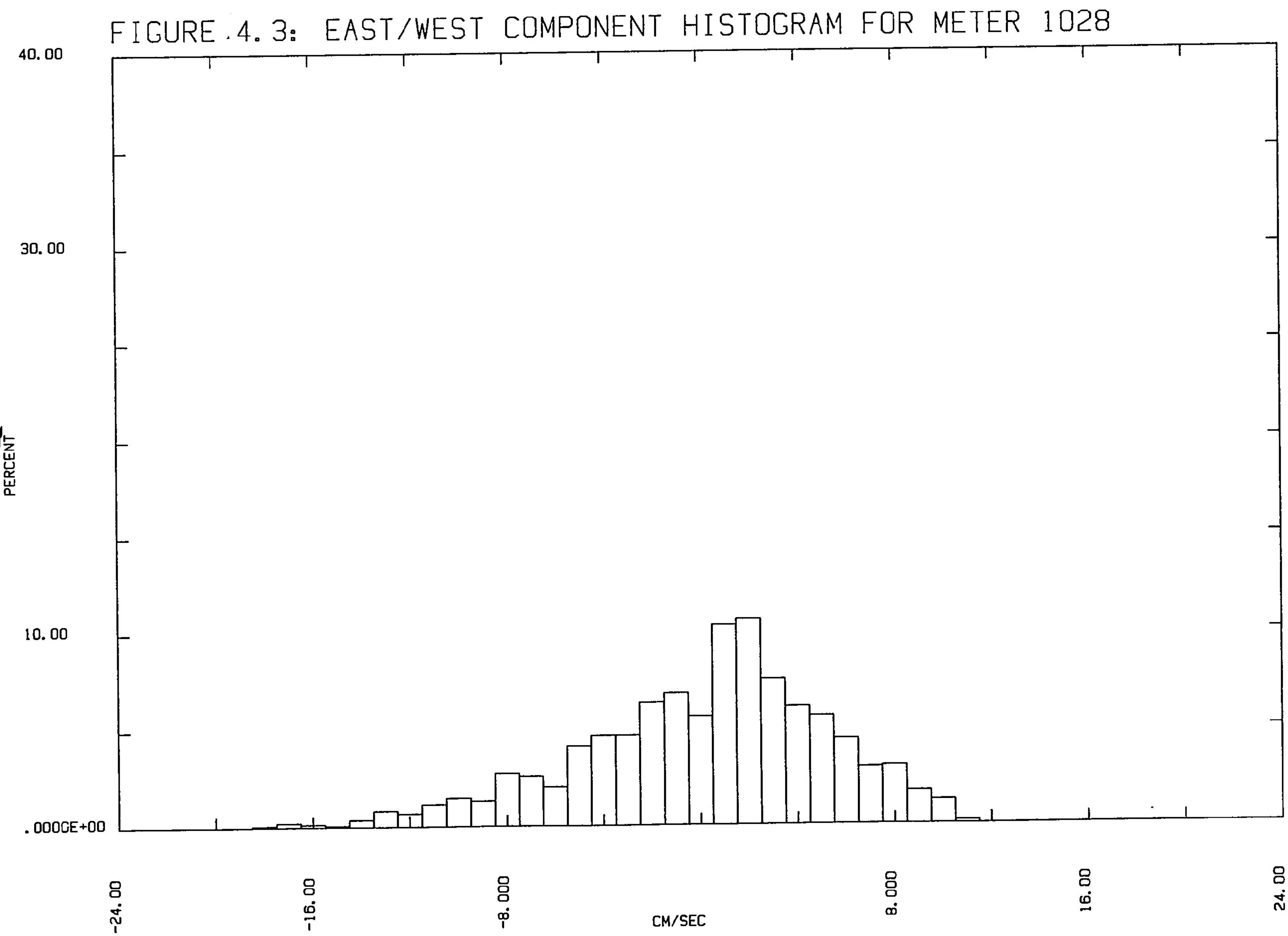
FIGURE 4.3: EAST/WEST COMPONENT HISTOGRAM FOR METER 1028
40.00
30.00
10.00
.0000E+00
PERCENT
-24.00
-16.00
-8.000
8.000
16.00
24.00
CM/SEC

FIGURE 4.4: NORTH/SOUTH COMPONENT HISTOGRAM FOR METER 1028

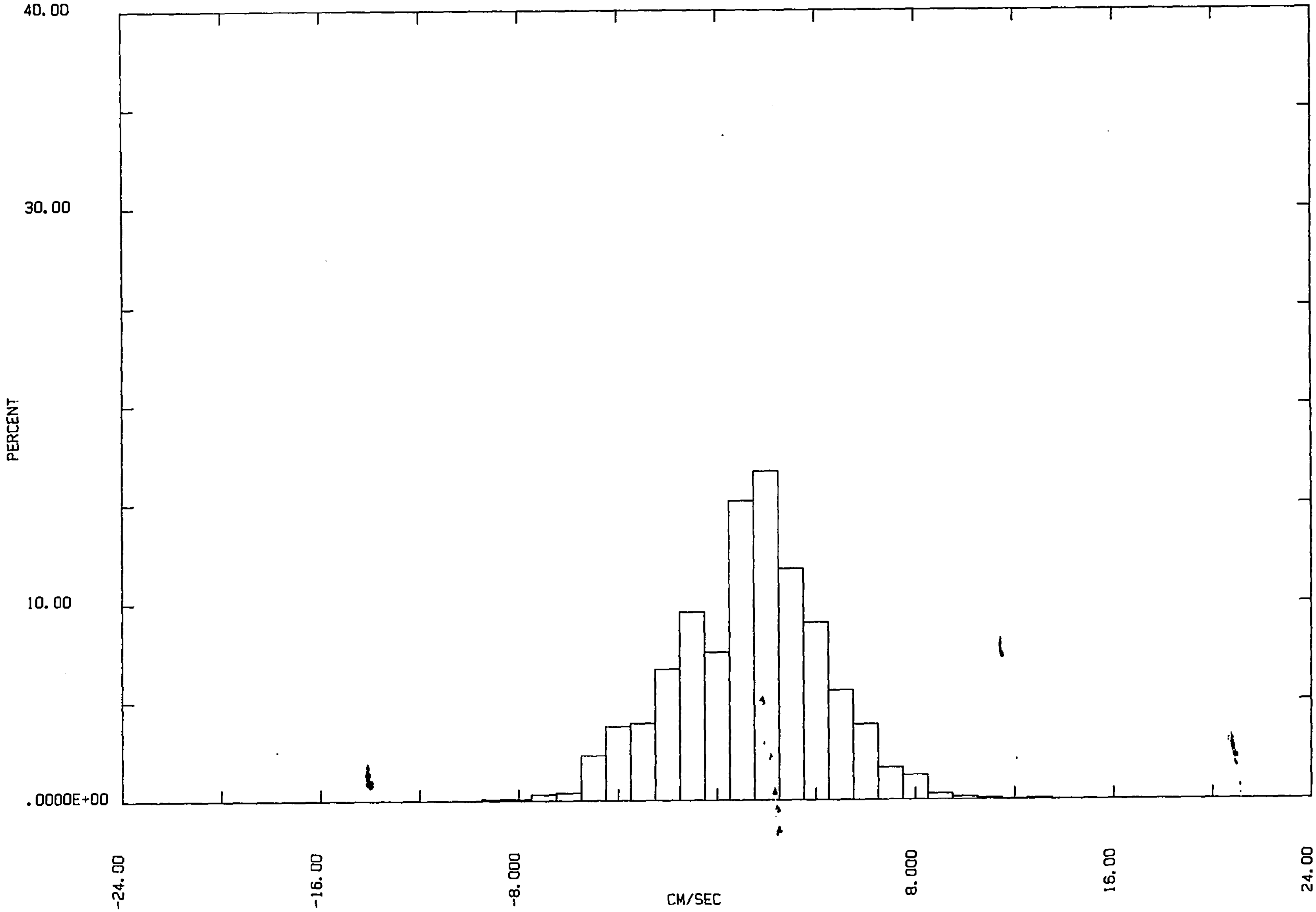

FIGURE 4.5: SCATTER DIAGRAM FOR METER 1028
SPEED VERSUS DIRECTION

X SCALE: DIRECTION (DEG. TRUE) FROM 0.0 TO 360.0 WITH 22.5 DEG. PER CLASS INTERVAL
Y SCALE: SPEED (CM/SEC) FROM 0.0 TO 19.00 WITH 1.0 CM/SEC PER CLASS INTERVAL

	.0	22.5	45.0	67.5	90.0	112.5	135.0	157.5	180.0	202.5	225.0	247.5	270.0	292.5	315.0	337.5	360.0
19.0	0	0	0	0	0	0	0	0	0	0	0	0	0	1	0	0	0
18.0	0	0	0	0	0	0	0	0	0	0	0	1	0	0	0	0	0
17.0	0	0	0	0	0	0	0	0	0	0	0	0	3	0	0	0	0
16.0	0	0	0	0	0	0	0	0	0	0	0	1	1	0	0	0	0
15.0	0	0	0	0	0	0	0	0	0	0	0	6	2	0	0	0	0
14.0	1	0	0	0	0	0	0	0	0	0	0	4	1	0	0	0	0
13.0	0	1	3	0	0	0	0	0	0	0	0	5	2	1	0	0	0
12.0	0	0	4	0	0	0	0	0	0	0	1	7	3	0	0	2	0
11.0	0	1	14	1	0	0	0	0	0	0	1	11	8	0	0	1	0
10.0	1	4	17	6	0	0	0	0	0	0	1	5	5	2	1	0	0
9.0	0	4	29	8	0	0	0	0	0	1	3	15	7	2	3	2	0
8.0	2	0	28	6	2	0	0	0	0	0	4	19	10	3	5	1	4
7.0	4	4	20	6	2	0	0	0	0	0	2	4	5	1	2	5	2
6.0	7	10	32	21	1	0	1	0	0	2	8	9	7	5	2	4	7
5.0	8	15	32	27	7	3	0	2	1	4	5	20	14	9	5	6	8
4.0	7	10	41	12	7	3	0	1	7	0	6	17	11	10	8	10	10
3.0	17	11	18	17	8	2	2	4	0	5	5	4	5	10	11	12	8
2.0	23	14	34	25	19	5	8	13	2	5	9	3	7	12	12	14	17
1.0	11	6	22	9	5	3	2	2	1	1	5	3	0	1	7	3	15
.0	8	3	11	3	1	0	0	2	0	0	2	0	0	2	0	0	0

TOTAL NUMBER OF POINTS: 1275.0

FIGURE 4.6: SCATTER DIAGRAM FOR METER 1028
NORTH/SOUTH VERSUS EAST/WEST COMPONENT

X SCALE: EAST/WEST COMPONENT (CM/SEC) FROM -19.00 TO 19.00 WITH 2.0 CM/SEC PER CLASS INTERVAL
Y SCALE: NORTH/SOUTH COMPONENT (CM/SEC) FROM -19.00 TO 19.00 WITH 2.0 CM/SEC PER CLASS INTERVAL

	-19.0	-17.0	-15.0	-13.0	-11.0	-9.0	-7.0	-5.0	-3.0	-1.0	1.0	3.0	5.0	7.0	9.0	11.0	13.0	15.0	17.0	19.0
19.0	0	0	0	0	0	0	0	0	0	0	0	0	0	0	0	0	0	0	0	0
17.0	0	0	0	0	0	0	0	0	0	0	0	0	0	0	0	0	0	0	0	0
15.0	0	0	0	0	0	0	0	0	0	0	0	0	0	0	0	0	0	0	0	0
13.0	0	0	0	0	0	0	0	0	0	0	0	1	1	0	0	0	0	0	0	0
11.0	0	0	0	0	0	0	0	1	0	0	0	0	1	0	0	0	0	0	0	0
9.0	0	0	0	0	0	0	2	1	3	1	0	5	3	3	2	0	0	0	0	0
7.0	0	0	0	0	0	0	3	4	5	6	11	8	5	8	8	4	0	0	0	0
5.0	1	0	0	0	0	2	3	8	10	17	17	24	25	28	24	10	0	0	0	0
3.0	0	0	0	1	1	3	2	5	37	49	64	51	42	27	16	3	0	0	0	0
1.0	0	1	0	1	4	3	10	19	35	34	87	73	46	20	0	1	0	0	0	0
-1.0	0	3	3	4	9	14	11	33	28	15	19	36	15	4	1	0	0	0	0	0
-3.0	0	0	0	8	9	14	19	17	11	13	23	2	3	0	0	0	0	0	0	0
-5.0	0	1	4	0	11	9	7	8	6	7	5	2	0	0	0	0	0	0	0	0
-7.0	0	0	1	4	0	1	1	1	0	1	0	0	0	0	0	0	0	0	0	0
-9.0	0	0	0	0	0	1	0	1	0	0	0	0	0	0	0	0	0	0	0	0
-11.0	0	0	0	0	0	0	0	0	0	0	0	0	0	0	0	0	0	0	0	0
-13.0	0	0	0	0	0	0	0	0	0	0	0	0	0	0	0	0	0	0	0	0
-15.0	0	0	0	0	0	0	0	0	0	0	0	0	0	0	0	0	0	0	0	0
-17.0	0	0	0	0	0	0	0	0	0	0	0	0	0	0	0	0	0	0	0	0
-19.0	0	0	0	0	0	0	0	0	0	0	0	0	0	0	0	0	0	0	0	0

TOTAL NUMBER OF POINTS: 1275.0

FIGURE 4.7: SCATTER DIAGRAM
SPEED FOR METER 1009 VERSUS SPEED FOR METER 1028

X SCALE: SPEED-1028 (CM/SEC) FROM 0.0 TO 19.00 WITH 1.0 CM/SEC PER CLASS INTERVAL
Y SCALE: SPEED-1009 (CM/SEC) FROM 0.0 TO 19.00 WITH 1.0 CM/SEC PER CLASS INTERVAL

	.0	1.0	2.0	3.0	4.0	5.0	6.0	7.0	8.0	9.0	10.0	11.0	12.0	13.0	14.0	15.0	16.0	17.0	18.0	19.0
19.0	0	0	0	0	0	1	0	0	0	0	0	0	0	0	0	0	0	0	0	0
18.0	0	1	0	0	1	1	0	0	1	1	0	0	0	0	0	0	0	0	0	0
17.0	0	0	1	0	0	1	1	0	0	0	0	0	0	0	0	0	0	0	0	0
16.0	0	0	4	0	0	2	1	0	0	1	1	0	0	0	0	0	0	0	0	0
15.0	0	0	1	1	3	1	0	0	0	0	1	1	0	0	0	0	0	0	0	0
14.0	0	1	1	4	0	1	3	2	1	0	0	1	0	0	0	0	0	0	0	0
13.0	1	2	3	4	0	0	6	5	1	1	0	1	0	0	0	0	0	0	0	0
12.0	0	2	6	1	5	7	1	2	2	6	0	0	0	1	0	1	0	0	0	0
11.0	1	1	3	4	2	5	6	0	1	1	1	1	0	0	1	0	0	0	0	0
10.0	2	2	8	3	4	6	7	3	3	2	0	1	0	2	0	0	0	0	0	0
9.0	2	3	16	3	5	7	4	3	4	4	3	0	0	1	0	1	0	0	0	0
8.0	1	5	10	7	5	10	5	2	6	2	0	1	2	1	0	2	0	1	0	0
7.0	3	8	20	5	10	12	11	1	5	5	2	2	2	0	2	0	2	0	1	0
6.0	2	8	16	14	15	13	9	4	10	5	3	3	2	3	0	1	0	1	0	0
5.0	3	4	29	18	14	18	10	10	11	6	2	3	1	0	0	0	0	0	0	0
4.0	3	16	23	11	22	20	11	7	7	14	8	5	2	1	1	1	0	0	0	1
3.0	6	24	30	25	39	25	22	10	15	11	9	9	3	1	2	0	0	0	0	0
2.0	7	14	32	32	21	22	8	6	14	10	8	3	3	1	0	2	0	0	0	0
1.0	1	2	15	6	12	9	7	1	3	5	4	5	1	1	0	0	0	1	0	0
.0	0	3	4	1	2	5	4	1	0	0	0	1	1	0	0	0	0	0	0	0

TOTAL NUMBER OF POINTS: 1275.0

4.4 Time History Records

Time history plots were produced for the speed records for both meters, and for the two speed component records for meter 1028. The time history for meter 1009 included 1286 half-hour samples, while the histories associated with meter 1028 consisted of 1278 samples. 1275 time points were common to both meters.

The speed record for meter 1028 essentially reproduces the information previously given by Schwartzlose, except that the format is changed to allow presentation of the entire record on one plot (Figure 4.8). The envelope of the speed record shows peak events occurring toward the middle of the record (around 9/3-9/6 and 9/10/75) and at the end (9/16-9/17). Periods of relatively lower activity occur around 8/25-8/29 and 9/11-9/14. Most of the changes in the envelope are associated with changes in the east/west current speed, as shown by the east/west speed plot in Figure 4.9. The envelope peaks and lows are readily visible in Figure 4.9, but the north/south time history in Figure 4.10 is virtually stationary. The skewing of the east/west speed distribution to the west is very apparent in the time history plot, as it is in the corresponding histogram and moments summary. Also, the north/south time history shows a fairly visible northward bias, as previously noted from the histogram and moment summary associated with it.

The speed time history plot for meter 1009 (Figure 4.11) differs somewhat from the speed time history plot for 1028. The envelope shows peaks around 8/22-8/23, 8/31-9/2, 9/5-9/6, 9/9-9/13 and 9/17. Envelope lows are around 8/25-8/27 and 9/8. Comparing the envelope peaks and lows for the two meters indicates that the two records are in greatest contrast around 9/11 through 9/13, where meter 1009 shows peak activity while meter 1028 is recording relative lows. These differences are at least in part attributable to local topographical differences. Figure 3.1 shows meter 1028 to be located on the north side of a depression while 1009 is shown to be on the opposite slope.

4.5 Progressive Vector Diagram and Stick Plot for Current Meter No. 1028

Schwartzlose presented a progressive vector diagram for the speed and direction data taken from meter 1028 (Ref. 2). A separate vector plot was

FIGURE 4.8: TIME HISTORY PLOT OF SPEED FOR 1028

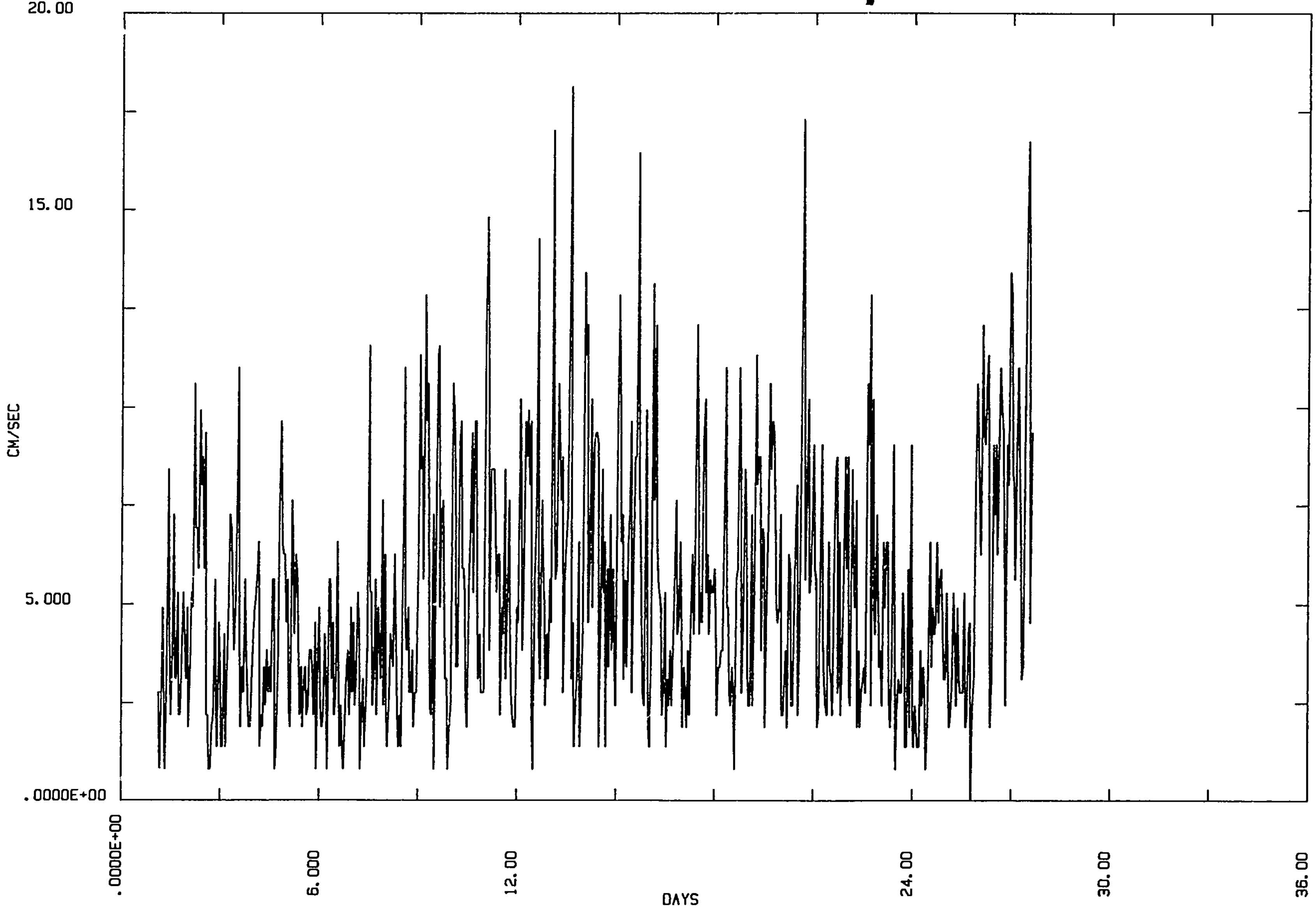

FIGURE 4.9: TIME HISTORY PLOT OF EAST SPEED COMPONENT FOR 1028

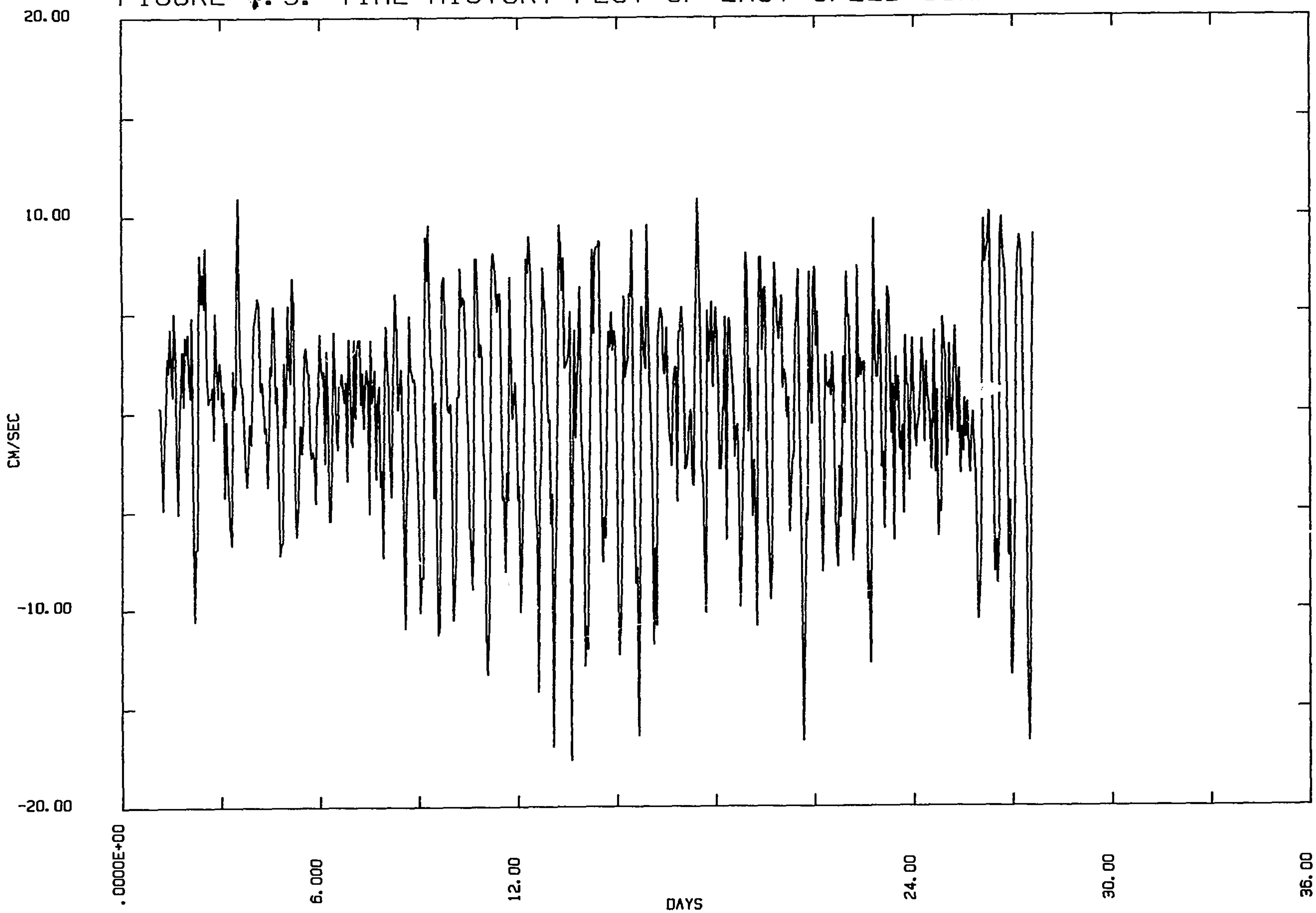

FIGURE 4.10: TIME HISTORY PLOT OF NORTH SPEED COMPONENT FOR 1028

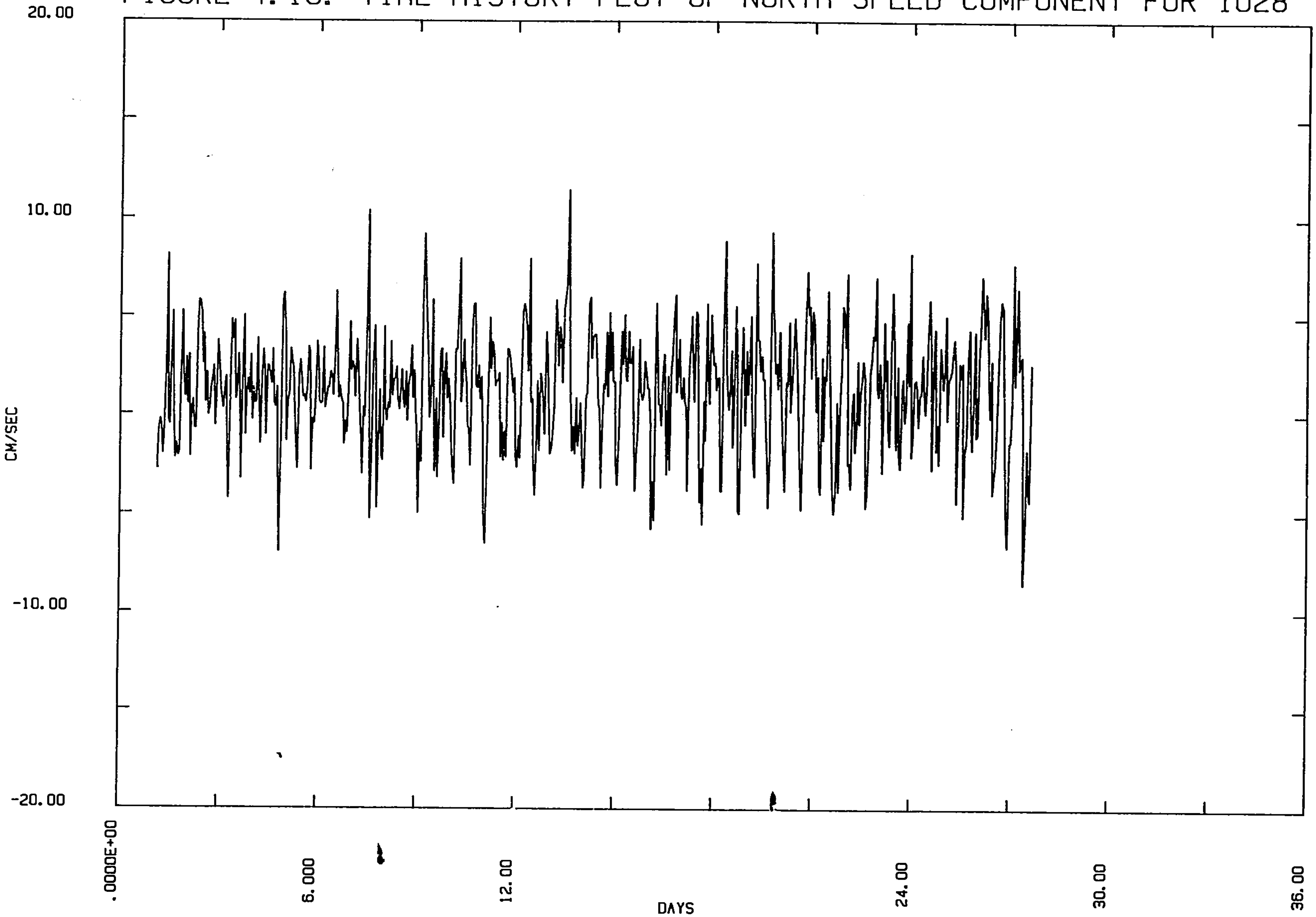

FIGURE 4.11: TIME HISTORY PLOT OF SPEED FOR 1009

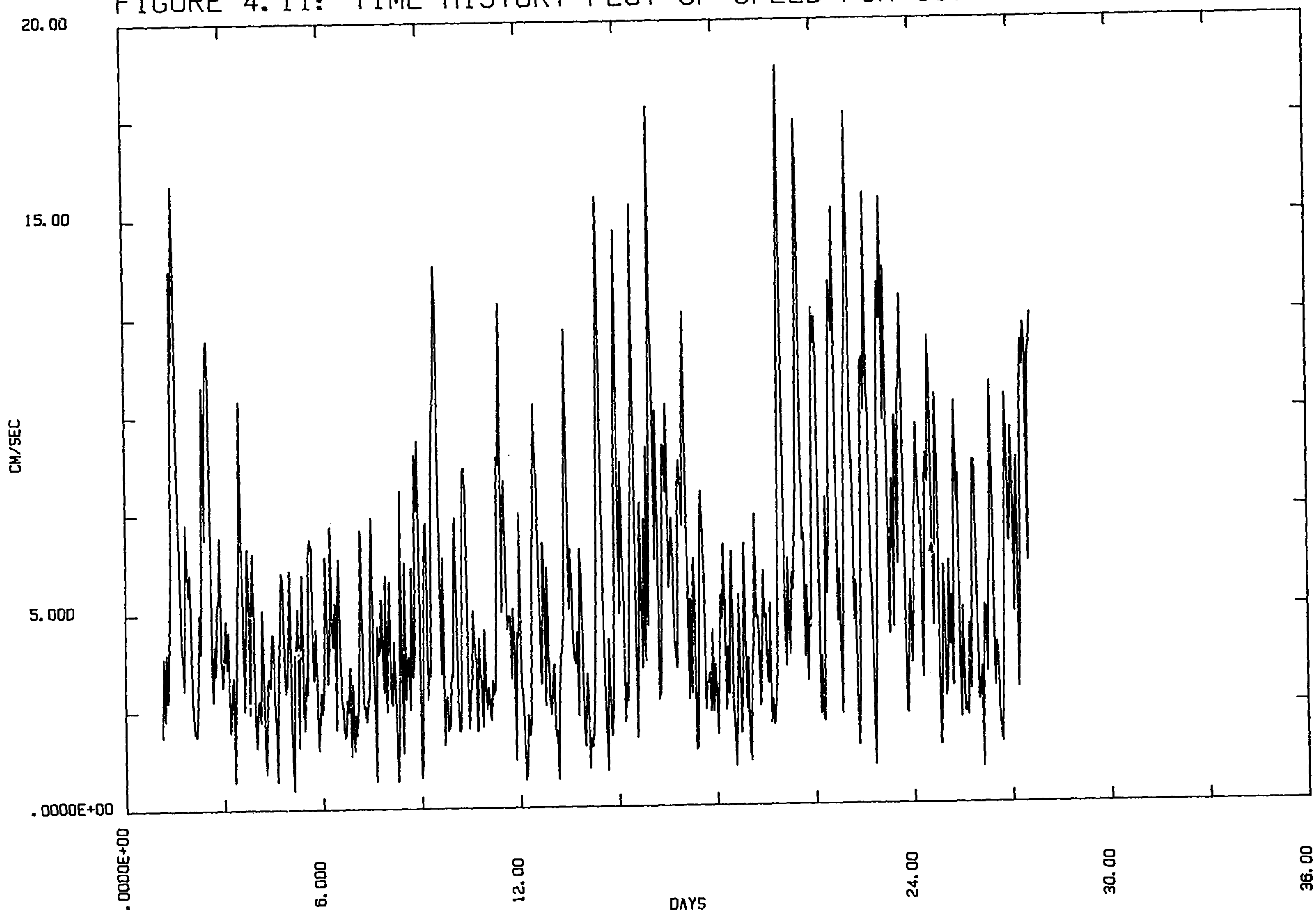

generated here (Figure 4.12) using the raw speed record, and was found to be the same as Schwartzlose's. The plot indicates a definite northward trend, with a mean speed of 1.33 cm/sec and a mean direction of 4° true. The tidal excursions are apparent in the plot, and were characterized by speeds of 4-8 cm/sec and excursion distances of about one kilometer.

The progressive vector plot was generated again for Figure 4.13, this time using digitally filtered speed component records in order to remove the tidal frequencies. The filter used was a cosine tapered symmetric finite impulse response filter with a cutoff frequency corresponding to a 50 hour period. This was the same filter used in the development of the progressive vector diagrams for the five meters in the 1977-1978 survey (Reference 4).

The vector-averaged current velocities for the 1977-1978 study and for meter 1028 are tabulated in Table 4.7. The similarity between 2919 and 1028 is readily apparent.

The stick plot for the filtered speed components for meter 1028 is given in Figure 4.14. This plot for the 27-day measurement period has been scaled to maximize the resolution of the velocity vectors, and clearly illustrates the predominance of northward flow during this measurement period. To convert the vectors shown in the plot to filtered speeds in cm/sec, multiply the length of the vector by the scaling factor of 4.63.

4.6 Coherence and Correlation Studies

In order to provide some initial insight into the periodic phenomena involved in the time records for meters 1009 and 1028, spectral density functions were obtained. The power spectral densities for the east/west and north/south current components for meter 1028 are shown in Figure 4.15 and 4.16, respectively. Power spectral densities were also obtained for the velocity for both 1028 (Figure 4.17) and 1009 (Figure 4.18). These plots provide an indication of the amount of current flow associated with the tides and other periodic current components. Spectral density estimates are not normally obtained for speed magnitude measurements since the result is biased due to the necessarily positive nature of the record. Also, harmonics are introduced

FIGURE 4.12: PROGRESSIVE VECTOR PLOT FOR 1028 RAW DATA RECORD

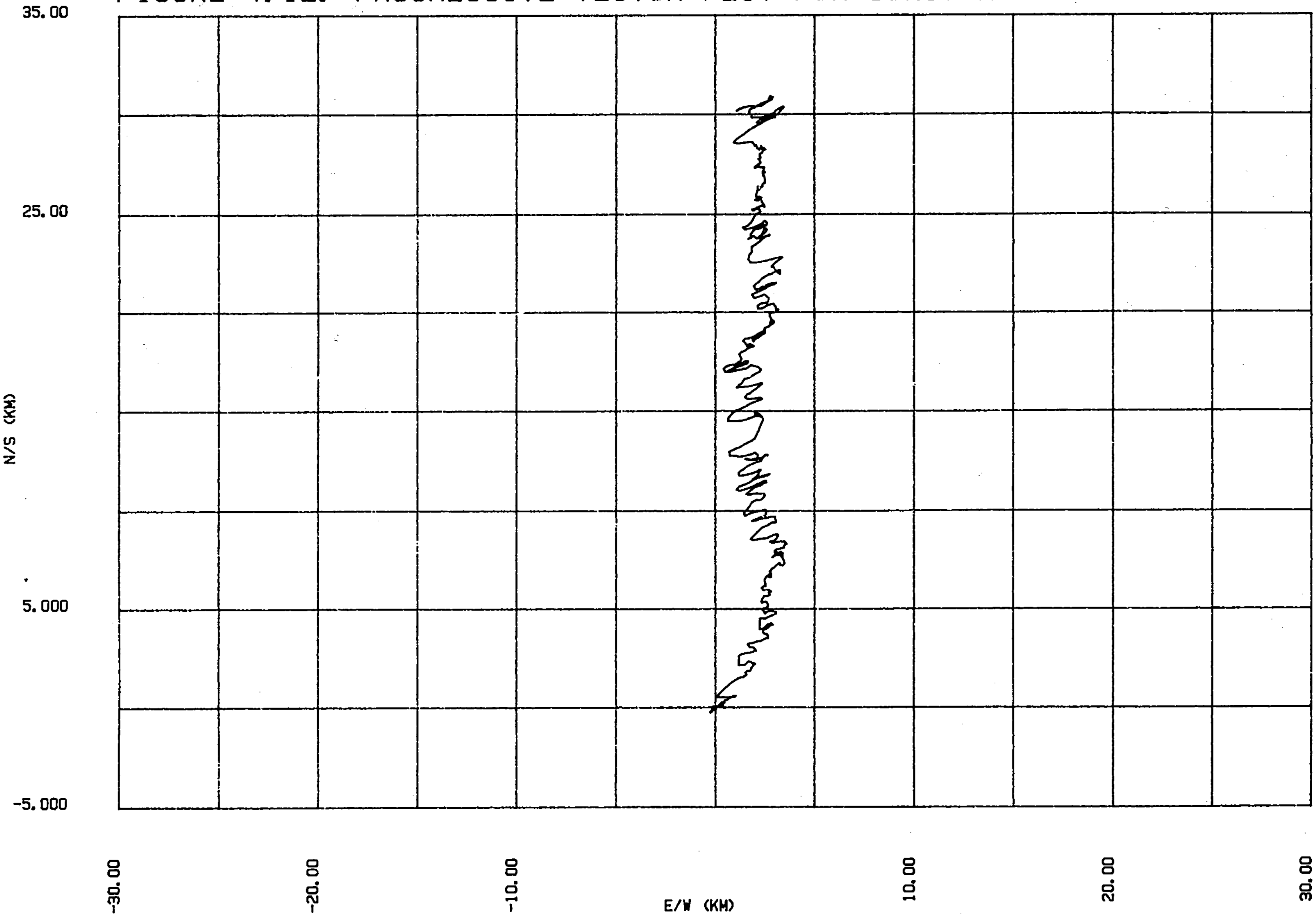

FIGURE 4.13: PROGRESSIVE VECTOR PLOT FOR FILTERED 1028 RECORD

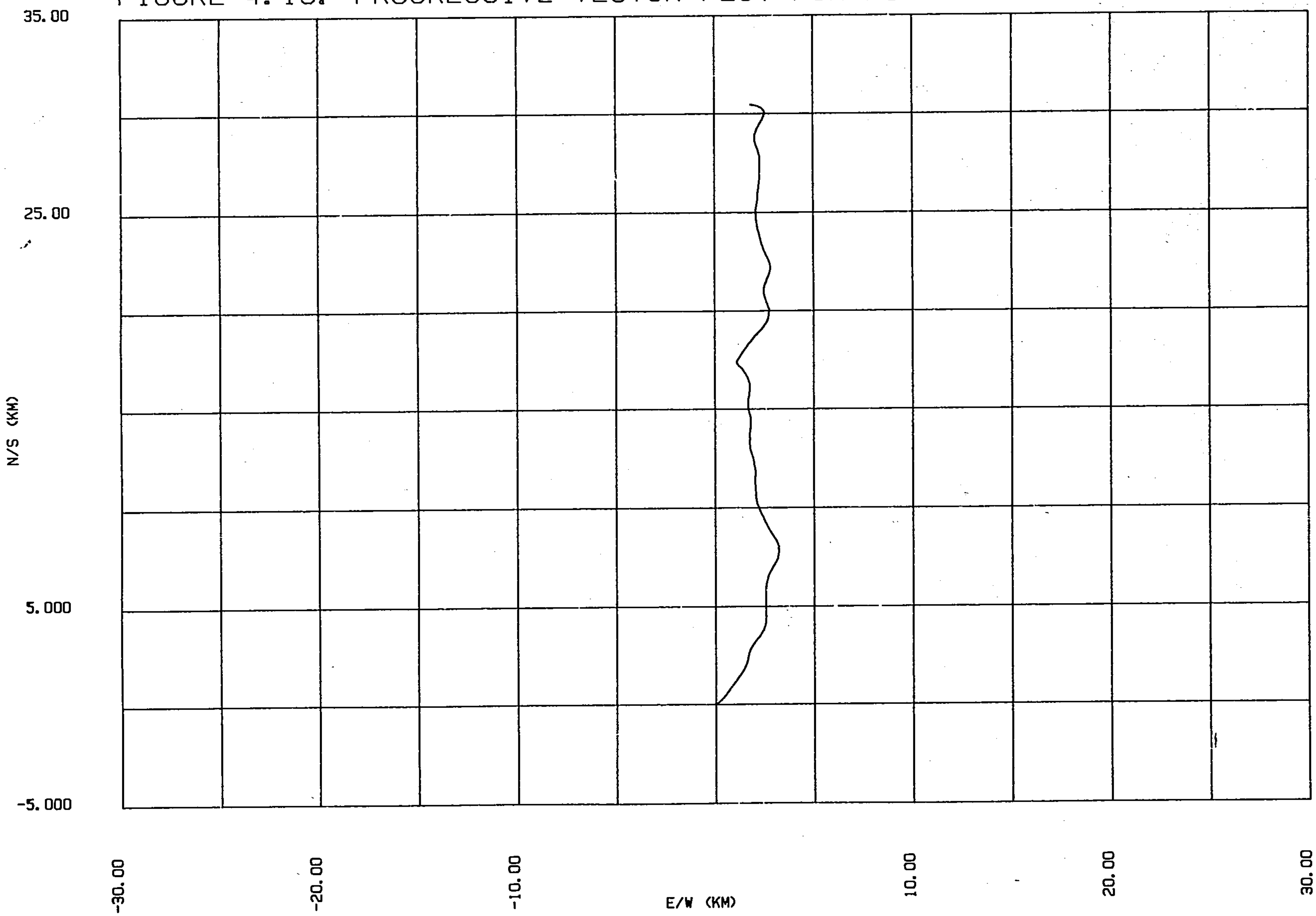

TABLE 4.7: VECTOR AVERAGED VELOCITIES

METER NO.	NOV'77 SPEED (cm/sec)	NOV'77 DIRECTION (deg. true)	DEC'77 SPEED	DEC'77 DIRECTION	TOTAL PERIOD SPEED	TOTAL PERIOD DIRECTION
2920	.23	-34.	.29	22.	.17	57.
2830	.56	-21.	1.92	144.	.67	137.
VACM	.98	-15.	1.84	164.	.90	152.
2918	1.48	74.	1.15	56.	1.40	69.
2919	1.82	14.	1.73	-2.	1.70	2.
1028	-	-	-	-	1.33	4.

FIGURE 4.14: STICK PLOT FOR FILTERED 1028 RECORD

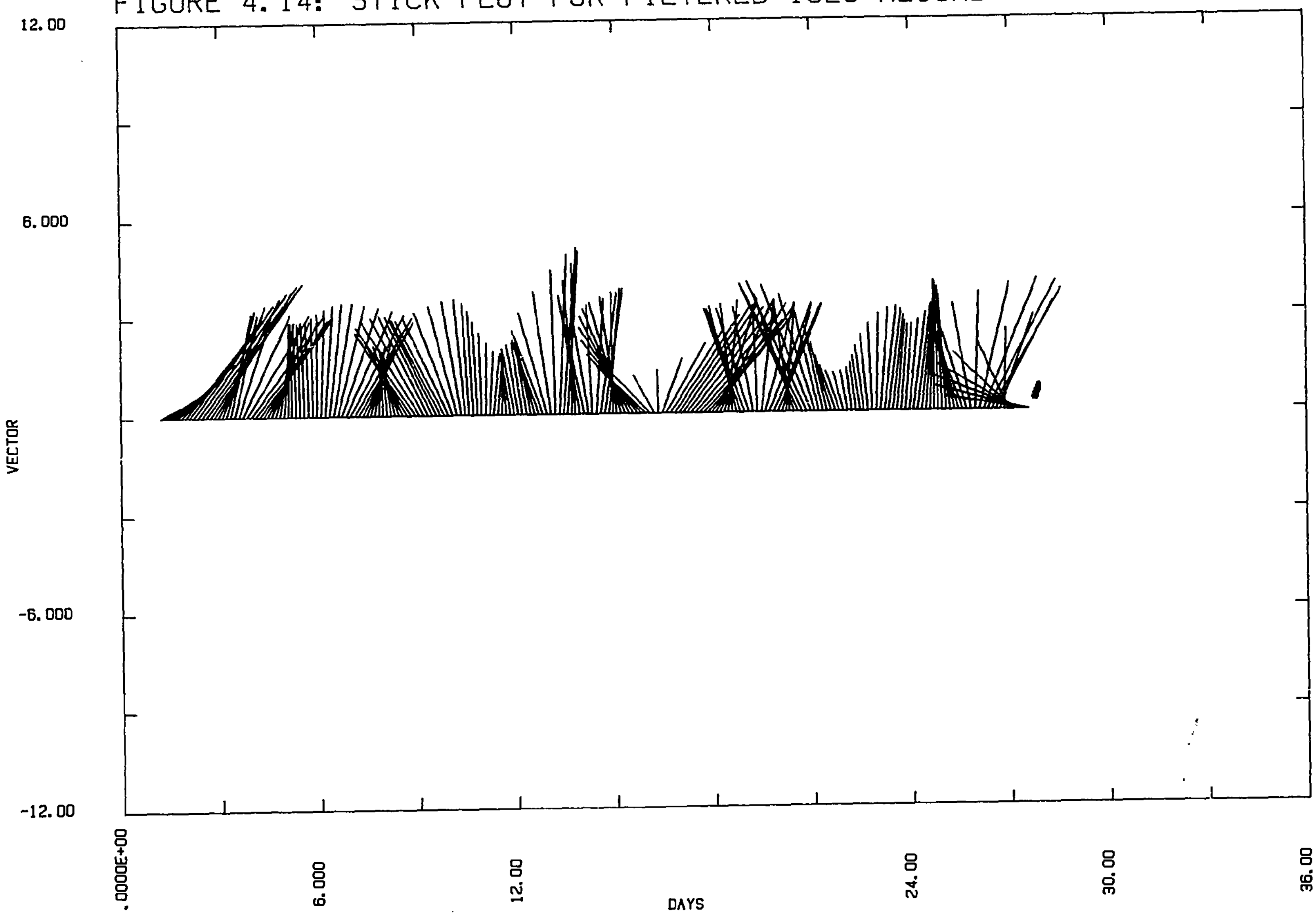

FIGURE 4.15: POWER SPECTRAL DENSITY FOR EAST COMPONENT FOR 1028

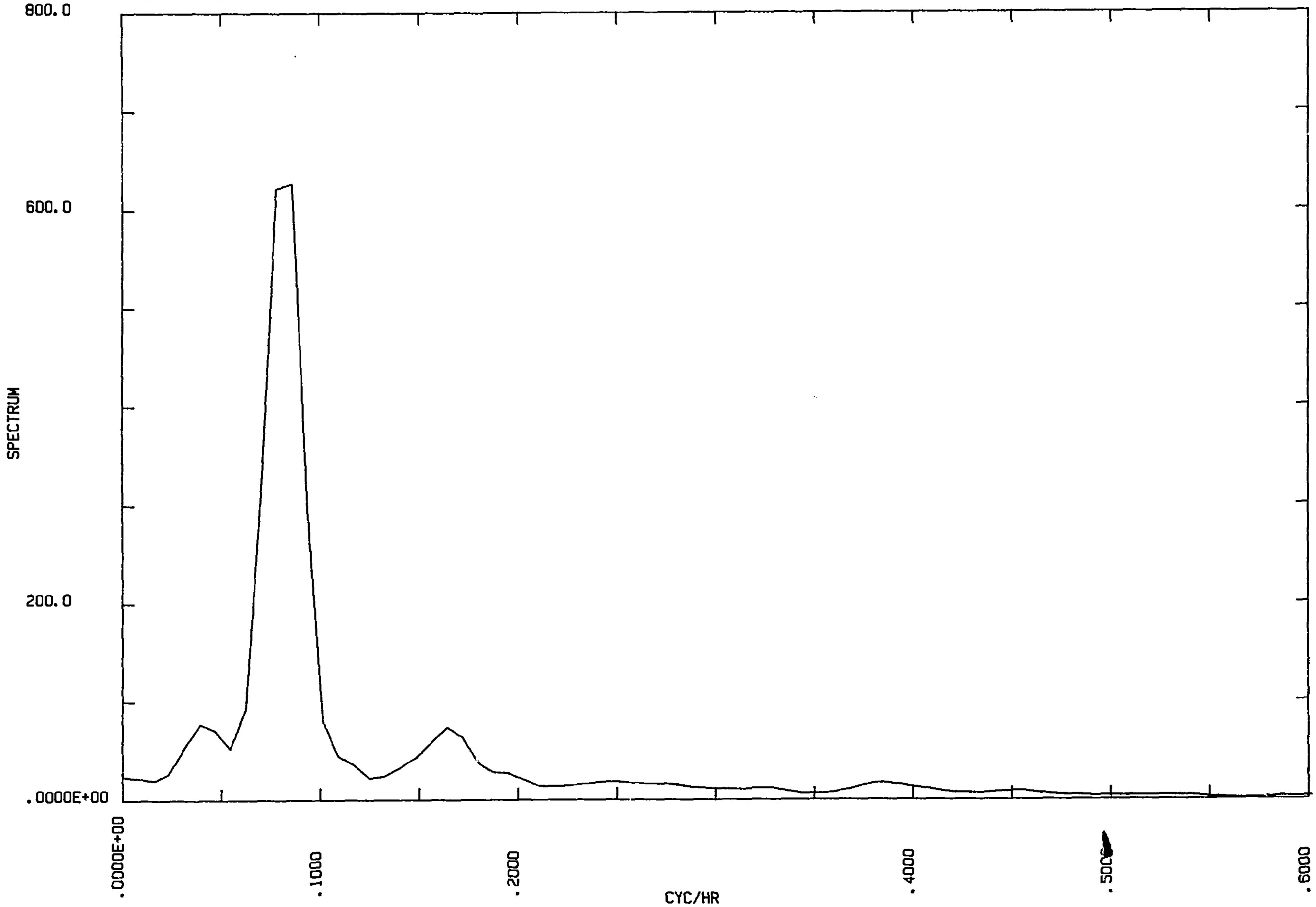

FIGURE 4.16: POWER SPECTRAL DENSITY FOR NORTH COMPONENT FOR 1028

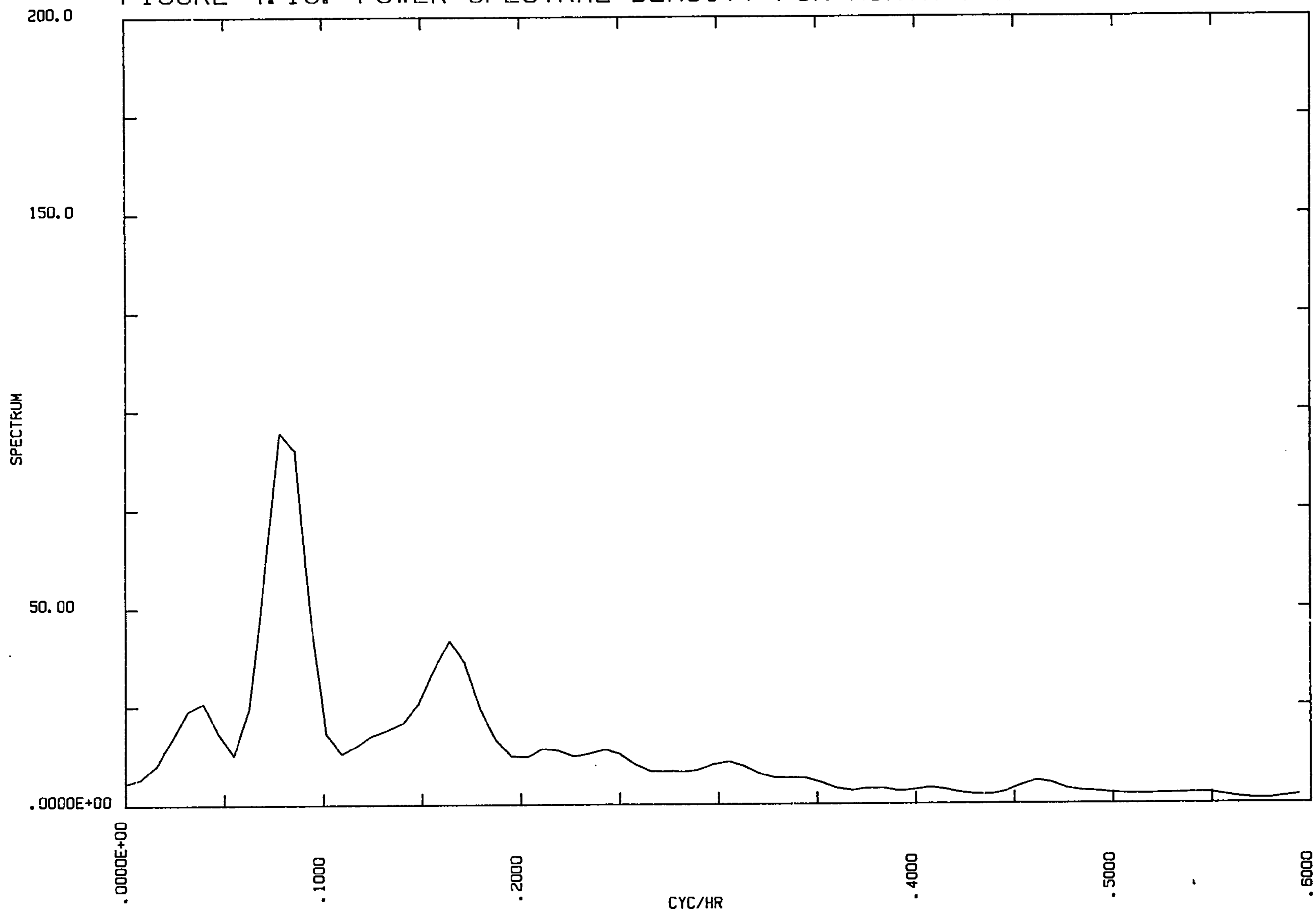

FIGURE 4.17: POWER SPECTRAL DENSITY FOR SPEED FOR 1028

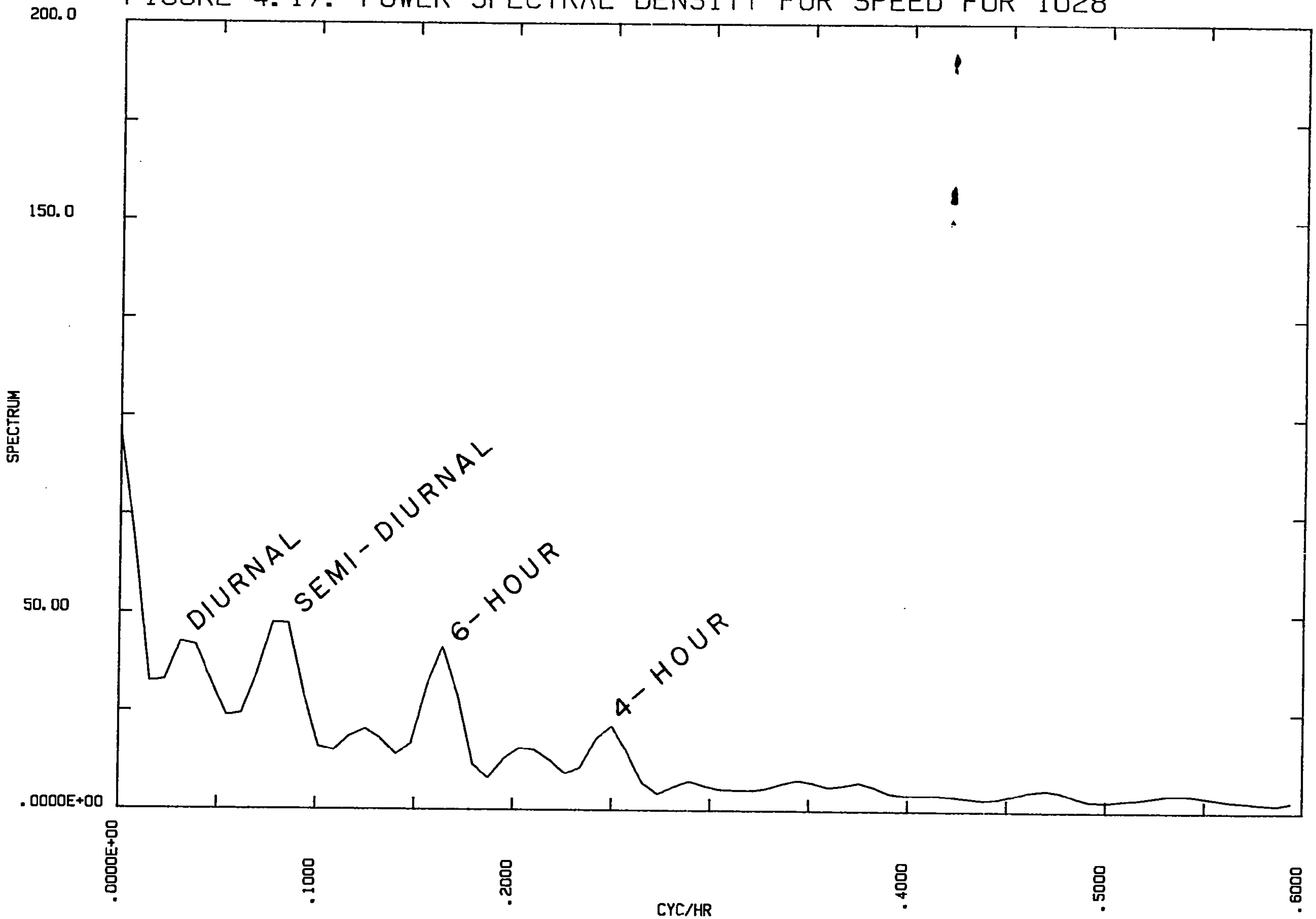

FIGURE 4.18: POWER SPECTRAL DENSITY FOR SPEED FOR 1009

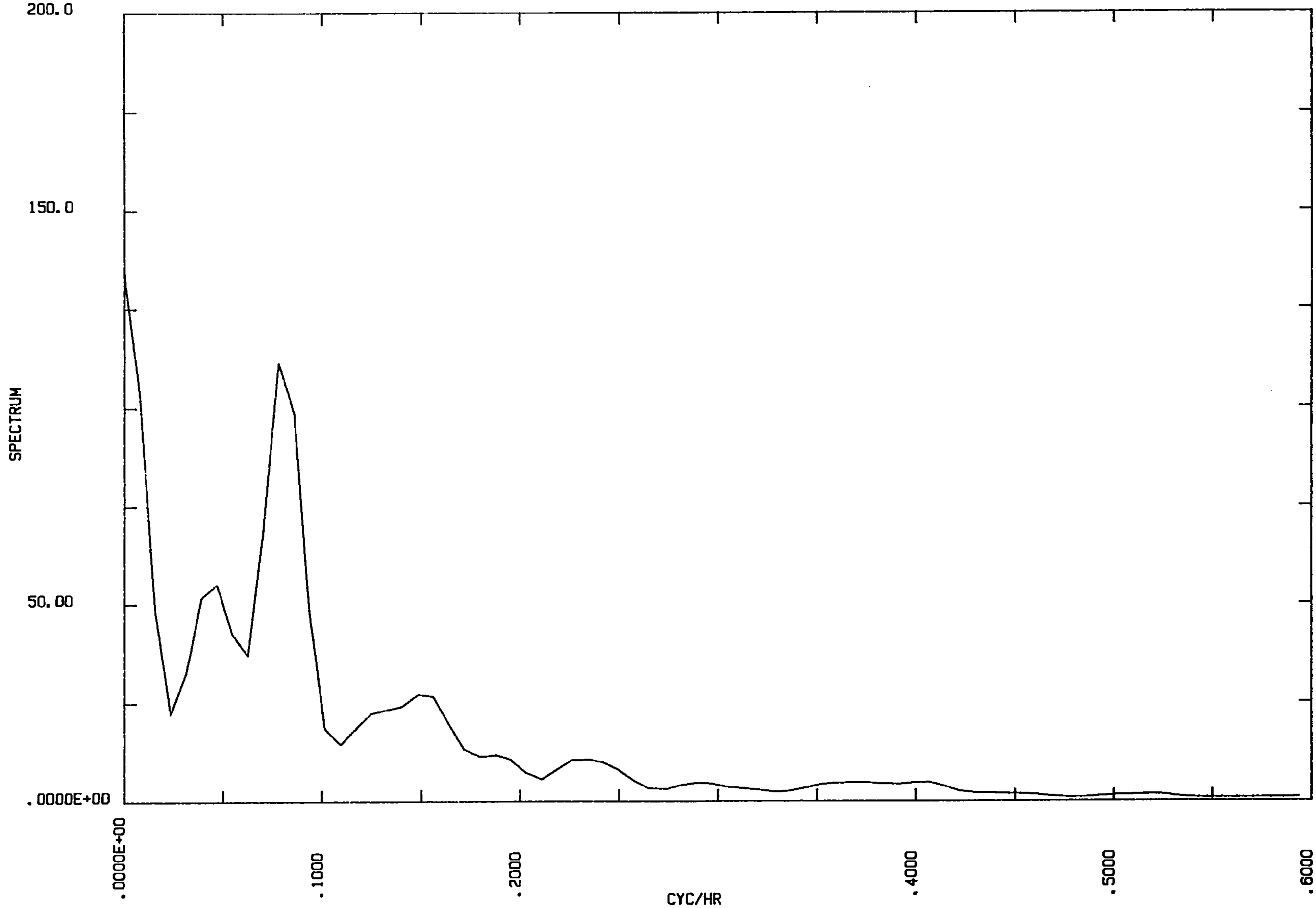

into the spectrum. However, since no directional information was available for meter 1009, this provided the only means of identifying spectral peaks for this meter. The spectral estimates obtained are useful for comparison.

The east/west component spectrum for 1028 is dominated by a sharp peak at the 12 hour semi-diurnal tidal frequency. Smaller peaks are apparent at the 24 hour diurnal frequency and at the 6 hour frequency. The north/south component reveals the same three peaks, but the semi-diurnal peak is not nearly so dominating, and the diurnal frequency is proportionally larger.

The spectrum of speed for meter 1028 (Figure 4.17) shows a bias component at zero frequency and four main spectral peaks. Ranked in decreasing order of size, these are the semi-diurnal tide, diurnal tide, a 6-hour peak, and a 4-hour peak. Since the 4-hour peak is not observed in either of the component spectra, it is probably just a numerical artifact at the second harmonic of the semi-diurnal tide. In addition, the 6-hour peak contains some energy from the first harmonic.

The speed magnitude spectrum for meter 1009 (Figure 4.18) also contains the bias peak, and peaks at the four frequencies noted above, with the size decreasing in the same order. However, the semi-diurnal tide is relatively much larger. This suggests that currents recorded at this meter were more influenced by tidal phenomena than those measured by 1028.

A magnitude squared coherence function was produced for the velocity spectra for the two meters, and is given in Figure 4.19. The plot indicates relatively low coherence except at the low-frequency end of the spectrum. This, however, is mostly due to the presence of bias in the spectra caused by using the velocity magnitudes instead of orthogonal components. The other coherence peaks occur in the regions of the diurnal tides (and inertial frequency) and around the semi-diurnal tides. Neither of these peaks suggest strong coherences between the two meters, but there is some measure of consistency.

Since the two meters discussed above, 1009 and 1028, were displaced in time by more than 2 years (as well as having been deployed at different depths and having had different local bathymetric conditions) from the meters of the 1977-1978 deployment, no major coherences would be anticipated between the two

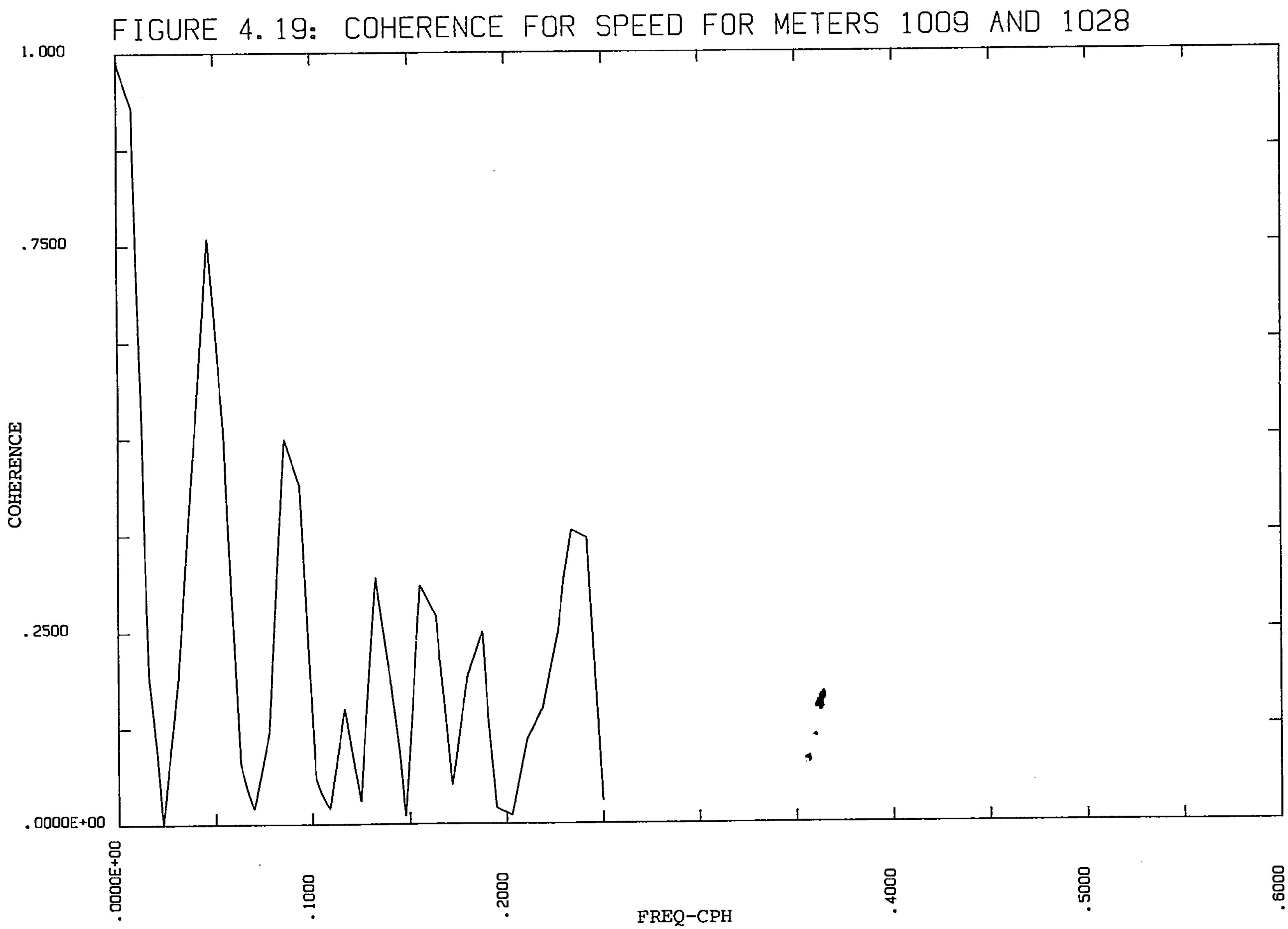
FIGURE 4.19: COHERENCE FOR SPEED FOR METERS 1009 AND 1028
1.000
.7500
.2500
.0000E+00
COHERENCE
.0000E+00
.1000
.2000
.4000
.5000
.6000
FREQ-CPH

measurement programs. In fact, even within the 1977-1978 deployment very little coherence could be discerned between any of the five meters, except in very narrow bandwidths around the tidal energies, and except for the meters which were deployed on the same arrays. However, general lower-order statistical relationships are observable between all seven meters, and these relationships are discussed in the next section.

SECTION 5

DATA INTERPRETATION

This section attempts to integrate the results of the analyses performed in the previous section with (1) the results of the analyses performed on the data collected with the five meters deployed in 1977-1978, and (2) general information on oceanographic phenomena within the Farallon Islands area. The current field in the area is characterized based on these results.

5.1 General Comments on Current Meter Hardware

Three types of current meters were used during the two measurement programs: Aanderaa meters, a Vector Averaging Current Meter, and the Scripps meters used in the 1975 deployment. All three meters are based on a Savonius rotor with directional readings recorded relative to magnetic north by means of a potentiometric compass. Consequently all three meter types produced speed records in terms of some digital revolution count of the rotor. The main physical differences in the meters relate to the means of determining current direction. The Aanderaa and Scripps meters used a large vane mounted behind the rotor which causes the rotor to always be pivoted into the oncoming current. The VACM uses a separate magnetically-coupled vane mounted above the rotor. Also, the VACM performs inter-sample vector averaging on the record, a process which is believed to help filter out high-frequency oscillations caused by mooring motions.

As for the records themselves, the major differences resulted from different sample rates. The VACM sampled at 4 samples/hour, the five Aanderaa meters each sampled at 3 samples/hour, and the two Scripps meters at 2 samples/hour. It should be noted, however, that the Scripps meters actually returned a continuous direction record since the recording medium was a strip chart. The velocity record was a quantized record by nature of the measurement mechanism. The sampling interval of one-half hour was chosen by the Scripps analysts when initial data reduction was performed by Dr. Schwartzlose on meter 1028. The nyquist rate of one sample/hour (i.e., the minimum sampling rate that must be used to avoid introducing aliasing errors) associated with the half-hour sampling interval (the slowest of the seven meters) was significantly higher than any energetic frequencies observed in any of the seven records.

5.2 Discussion of Relationships Observed between the 1975 and 1977-1978 Data

Some preliminary remarks may be made regarding the general nature of the currents near the Farallon Islands. The surface currents in the region are principally characterized by the California and the Davidson currents (Reference 5). These two currents flow counter to each other, the California current flowing southward with an average speed of approximately 25 cm/sec, and the Davidson current traveling northward either beneath the California current or at the surface closer to the shore. This second condition, when the Davidson current forms a wedge between the California current and the shore, occurs between mid-November and February. For the remainder of the year, the Davidson current runs at depths of greater than 200 meters at speeds of 10 to 40 cm/sec. Between mid-February and September, the California current carries surface water offshore and upwelling of deeper water occurs. The transition period, September to mid-November, following this upwelling period is characterized by ocean current patterns that are not well defined. This transition period occurs roughly during the period corresponding to the 1975 meter deployment. The 1977-1978 meter deployment began near the end of the transition period and continued into the surface period for the Davidson current, starting in mid-November. It is therefore evident that the two measurement programs obtained records of different phases of the current dynamics for two different years, a situation which severely limits the probability of finding specific correlations. For this reason, this discussion will be limited to observations on general relationships and general trends.

One apparent inconsistency observed regarding the 1975 deployment relates to the reported deployment locations and depths for the meters. The depths to which the meters were deployed were reported as being approximately 1849 m and 1729 m (both about 2 m above the bottom) for 1028 and 1009, respectively. In addition, 1009 was reported to be further west than any of the meters deployed in 1977-1978. The array which contained meters 2918 and 2919 was reported to be in water over 1800 m deep. This array was located fairly close to 1009 and, if anything, should have been in slightly shallower water. Thus it would appear that the discrepancy may be in the locations and/or depths reported in 1975. It is possible that these two meters were actually slightly east of the locations given, but if so, the discrepancy is not a large one. In any event, 1009 and 1028 were reportedly measuring currents just off the bottom, and this relationship will be assumed for the remainder of this discussion.

It is instructive to compare these two meters with the near-bottom meters 2919 and 2920. 2918 was also close to the bottom, having been approximately 26 m above 2919 on the same array. It was noted earlier, in Section 4.2, that the component statistical moments for 1028 and 2919 were notably close in character, both indicating mainly northward flow with a lesser shoreward component. The mean speeds for 1028 and 1009 were both within 20% of the mean speed for 2919 for the month of November, and this difference was diminished to less than 10% if the comparison was made using the first 6 days of the record (i.e., the final days of October) for 2919.

Meter 2918 was even closer in speed to 1009 and 1028 but the direction, although still in the northeast quadrant, was substantially different. In fact, the directional measurements for 2918 and 2919 appear to be inconsistent with each other, especially since they were only 26 m apart. However, the component minima, maxima and standard deviations were in close agreement. The discrepancy may have been due to a possible compass calibration error for 2918.

Meter 2920, which was located closest to shore of the seven meters, recorded somewhat reduced speeds relative to the other meters. It also showed very little consistency in average directional measurements, although there was some northward tendency. This meter may have been measuring dynamics close to the boundary of the surface California and Davidson currents, and consequently the behavior of the measured phenomena was not as well defined. The records from 1028 and 1009 were clearly more similar to those taken by 2919 and 2918 at the western end of the deployment region.

The array with the VACM and meter 2830 was reportedly deployed in 1372 m of water with the meters at a midwater depth of about 912 m. As noted in the report on the 1977-1978 analyses (Reference 4), the current vector reversed to a southeastward direction for these meters sometime around the end of November. However, during the northward phase the vector had a westward component. The average speeds, like the average speeds for 2918 and 2919, were a little larger (by about 20-25%) than the average magnitudes for the two 1975 meters.

Table 5.1 summarizes the mean speeds and vector average speeds for the seven meters.

Turning now to the periodic aspects of the data records, it was observed in Section 4.6 that both the east/west and north/south components of the speed record from 1028 are characterized by three major spectral peaks -- the semi-diurnal, diurnal, and a peak corresponding to roughly a 6-hour period. The semi-diurnal peak predominates in both components, especially in the east/west spectrum. The diurnal and 6-hour peaks are of about the same magnitude in the east/west spectrum, but the 6-hour peak has almost twice the energy of the diurnal peak in the north/south spectrum.

The November spectra for 2918 and 2919, provided in Reference 4 for these meters, tend to confirm the observations noted above for 1028. The east/west spectra for both of these meters show a dominant semi-diurnal peak followed by a much smaller (i.e., by a factor of 5) diurnal peak. A 6-hour peak of similar magnitude is observed in both spectra, and 2919 also contains a peak at about 8 hours. The north/south spectra are much less clearly defined, but in both of them the energy around the 6-hour peak is close in magnitude to the energy about the semi-diurnal tides. In the subsequent December, January and February north/south spectra for 2919 and 2918, the 6-hour peak emerges to become the dominating spectral energy. The emergence of this peak seems to be coincident with the surface phase of the Davidson current, suggesting that internal wave phenomena, connected with the interaction between the California and Davidson currents, are present.

Table 5.2 summarizes the spectral energy sources in the north/south and east/west current components of meter 1028.

TABLE 5.1: LONG TERM AVERAGES

METER NO.	MEAN SPEED (cm/sec)	EAST/WEST COMPONENT	NORTH/SOUTH COMPONENT	VECTOR AVERAGE SPEED	DIRECTION (deg. true)	COMPASS POINT
2920-OCT	4.16	.25	.48	.54	28.	NE
2920-NOV	4.77	-.13	.19	.23	-34.	NW
2830-OCT	6.46	-.55	.06	.55	-84.	W
2830-NOV	6.07	-.20	.52	.56	-21.	NNW
VACM-OCT	6.18	-.44	.56	.71	-38.	NW
VACM-NOV	6.73	-.26	.95	.98	-15.	NNW
2918-OCT	5.25	1.97	.61	2.06	73.	ENE
2918-NOV	6.35	1.42	.42	1.48	74.	ENE
2919-OCT	5.74	1.04	1.75	2.04	31.	NE
2919-NOV	6.58	.43	1.77	1.82	14.	NNE
1009-AUG/SEP	5.54	-	-	-	-	-
1028-AUG/SEP	5.26	.09	1.33	1.33	4.	N

TABLE 5.2: ENERGY COMPONENTS FOR METER 1028

PERIODIC ENERGY	FREQUENCY (cph)	EAST/WEST ENERGY $(cm/sec)^2$	NORTH/SOUTH ENERGY $(cm/sec)^2$
DIURNAL & INERTIAL CURRENTS	.04-.05	1.6	0.5
SEMIDIURNAL TIDES	.08-.083	12.9	1.8
SIX-HOUR SPECTRAL PEAK	.16-.175	1.5	0.8

5.3 Discussion of the Current Field

The seven current meter records discussed in the preceding section form the basis for estimating the nature of the current field neighboring the investigation area. The deployment geometry provides records at three points on the bottom, defining a triangular region in the horizontal plane. A fourth reference point is defined in the midwater column, located slightly south of the centroid of the horizontal triangle.

Figure 5.1 depicts graphically the vector-averaged current information given in Table 5.1. Note that no vectors are shown at the site of meter 1009 since this meter did not provide any directional record. The vectors shown at the other sites are the vector averages for October and November in the case of the 1977-1978 meters, and the vector average for the entire August to September record for meter 1028.

All of the vectors depicted are in the northern half of the compass. Almost all the vectors are predominantly northward, with the exceptions of the October and November vectors for 2918 and the October vector for 2830. It was noted earlier that meter 2918 seemed inconsistent regarding directional measurements, especially in view of its close proximity to 2919, and a miscalibrated compass was cited as a possible cause. The October vector for 2830 is not consistent with the VACM readings for the same period, but only six days of data are included in the October time period, and the measurements may contain some start-up transients. In any case, it is reasonably safe to say that, based on the measurements, the predominant flow through the area between August and November is northward. It also appears that the vector magnitudes decrease significantly as one proceeds up the continental shelf towards the shore. This decrease in vector magnitudes occurs in conjunction with a decrease in average current speeds, as indicated in Table 4.5. This suggests that the potential for suspended sediment transport from the dumpsite area progressively diminishes toward the eastern, or shoreward, end of the measurement site.

The prevailing surface currents through the region flow toward the south throughout most of the measurement period discussed here, which is consistent with the northward counterflows observed by the meters. However, some confusion

FIGURE 5.1: VECTOR AVERAGED LONG TERM CURRENTS

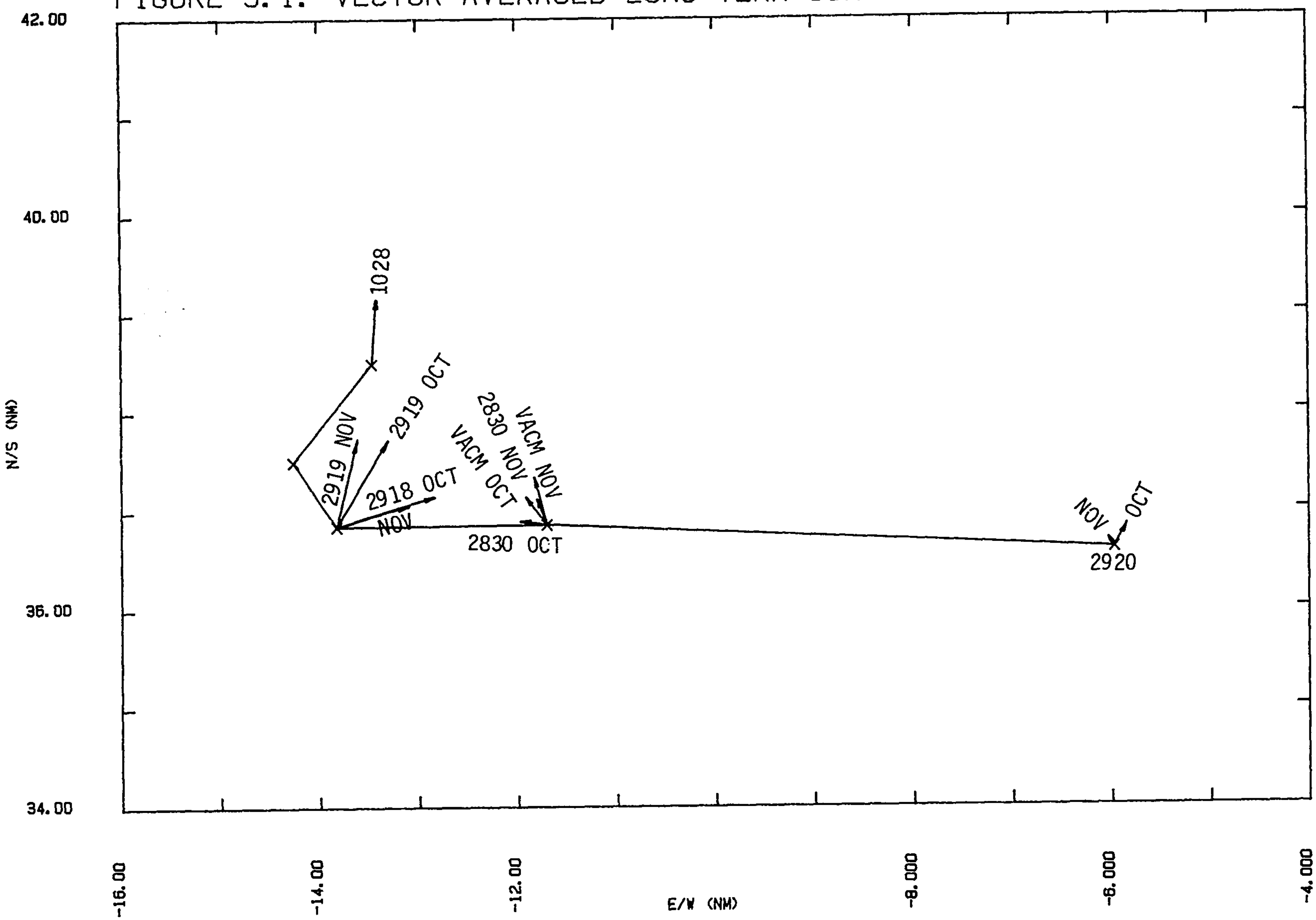

of direction occurs as the Davidson current surfaces toward the eastern part of the area in the latter part of November. As noted in Reference 4, a current direction reversal is observed in the midwater measurements at this time, and the measurements at the eastern end of the site do not show a very pronounced directional trend for any of the measurement period. The measurements taken by the seven current meters are reasonably consistent with the trends predicated by the hypothesis that they should observe flows counter to the surface currents. Also, the slight shoreward upslope flow observed at the western end of the site is reasonable in view of the shoreward direction of coriolis influences on the northward deepwater flow.

As discussed in Reference 4, a possible sediment transport mechanism might involve tidal and other periodic current components providing the impetus to suspend finer-grained sediment particles, with long term average currents sweeping the finer particles upslope and shoreward before they fall out of suspension. Reference 1 provides background on the nature of the sediments sampled in the dumpsite region. A hypothetical case was put forward in Reference 4 in which a particle which was only able to become suspended about 3% of the time (using 20 cm/sec as the threshold) at meter 2919, nevertheless remained in suspension about 85% of the time. The periodic current energy sources (particularly semi-diurnal tides) become large enough to make this possible, but the shoreward decay in vector averaged velocities noted above is matched by a shoreward decay in spectral energy magnitudes, thereby reducing the effectiveness of this mechanism with proximity to shore.

The major periodic energy sources, semi-diurnal tides, are depicted graphically as tidal ellipses in Figure 5.2. The majority of the energy in the deep western end of the site is east/west, as indicated by the shapes of the ellipses for meters 2918, 2919, and 1028. The midwater meters, 2830 and the VACM, have almost equal energies along the two orthogonal axes, with the maximum energy occurring along the northwest/southeast diagonal. Meter 2920 has slightly more energy in the north/south direction, with the maximum along the northeast/southwest diagonal. Meter 1028's ellipse more closely resembles those of the western deepwater meters 2918 and 2919 in terms of magnitudes, but it bears a closer resemblance in terms of orientation to the ellipse of meter 2920. This may be due to the possible misreporting of the location of

FIGURE 5.2: SEMI-DIURNAL TIDAL ELLIPSES

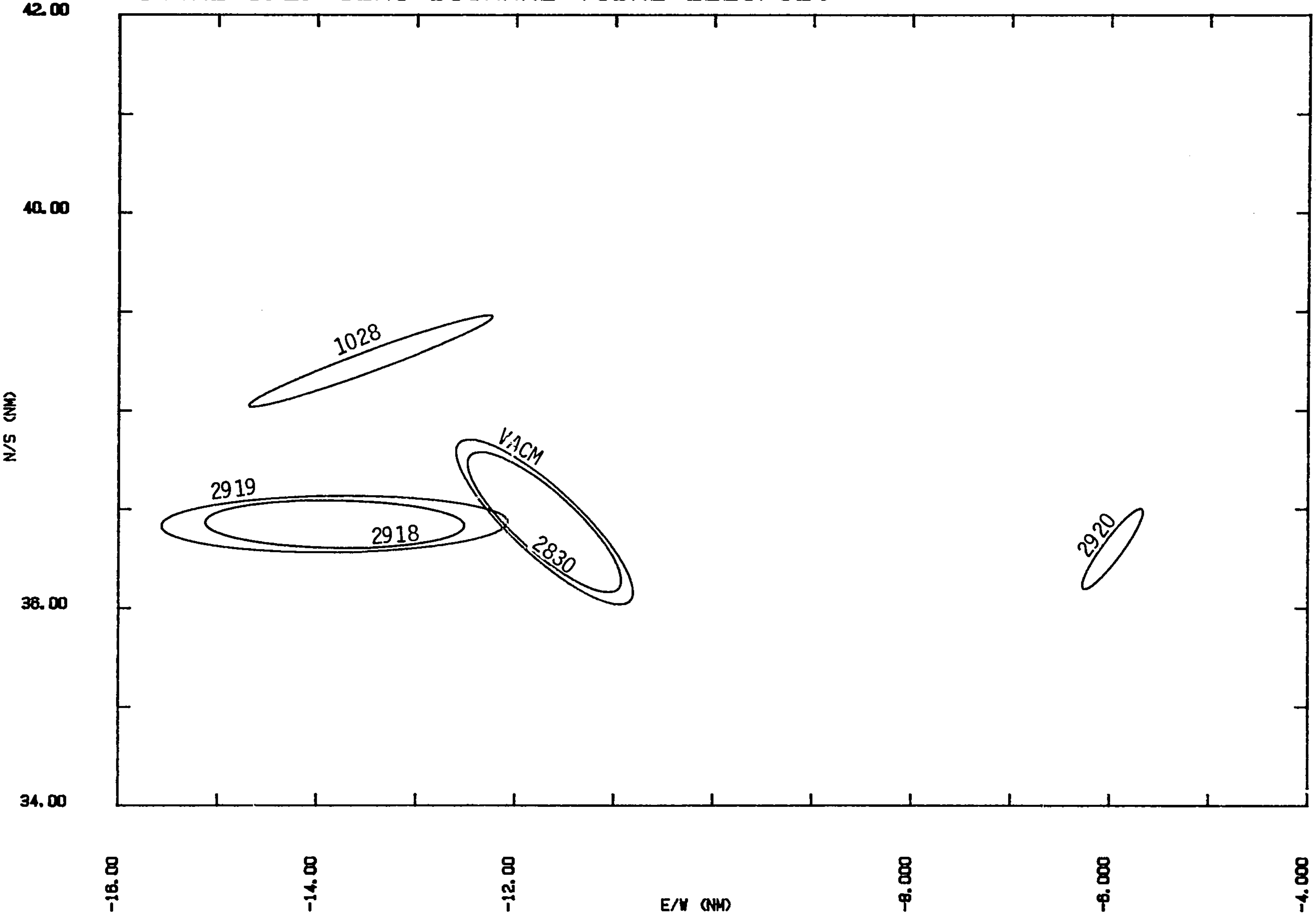

meter 1028, a possibility noted earlier in conjunction with an apparent inconsistency between the reported geographical coordinates and the reported depth. If this is the case, it seems likely that meter 1028 was actually located somewhat shoreward of the location shown in Figures 5.1 and 5.2.

Nevertheless, the major energy components are observed to be greatest toward the western end of the site, decreasing in magnitude toward the shore. Consequently, the potential for shoreward transport of suspended material appears to decrease significantly in the shoreward portion of the investigated region at least during the meter deployment periods. This decrease in transport potential is also supported by the observed velocity magnitudes and vector averages for the seven meters. It is therefore concluded that suspended transport from the dumpsite area during the months of August through November is a small but existent possibility, although additional measurements closer to shore and at other times of the year (particularly during upwelling) would be helpful in verifying this assessment.

SECTION 6

RESULTS AND CONCLUSIONS

The results and conclusions fall into four major categories: a) Overall Data Quality and Consistency, b) Specific Results for Meters 1009 and 1028, c) General Observations on the Local Current Field, and d) General Assessment of the Potential for Suspended Load Sediment Transport. Each of these categories is discussed below.

6.1 Overall Data Quality and Consistency

Data quality for the time periods under discussion, August/September 1975 and October/November 1977, was suitable for analysis. The data records were consistent and usable with the following qualifications:

- The data record for meter 1009 (August/September 1975) lacked directional reference due to a malfunction in the meter's compass.

- The reported geographical coordinates and the reported deployment depths for meters 1009 and 1028 were somewhat inconsistent with published bathymetry and with the bathymetry determined for the 1977-1978 survey of the Farallon area dumpsites. It is possible that the two meters were located somewhat shoreward of the reported coordinates.

- In the 1977 deployments within the same area (Reference 4), meter 2918 yielded vector-averaged velocities that were 60 to 70 degrees offset to the east from those of meter 2919. These meters were located on the same mooring only 26 m apart. It appears that the direction measurements for 2918 may not have been properly calibrated. Although a hydrographic station near the site of current meter 2918 and 2919 deployments was occupied in October 1977 (Reference 1), no anomalous water properties were observed in the near-bottom samples that could suggest that different water masses were responsible for the directional disparity within the 26 meter distance separating the two instruments.

- As noted in Reference 4, the record for meter 2830 had a dropout of about 9 hours at the beginning of the October deployment period. The VACM time sequence was jumbled, but the records of interest were rectified by matching them with the 2830 records since these two meters were located only 2 m apart on the same mooring.

6.2 Results for Meters 1009 and 1028

The speed for meter 1009 ranged between 0.0 and 20.61 cm/sec, with a mean magnitude of 5.54 cm/sec. For meter 1028, the range was 0.0 to 18.15 cm/sec, with a mean magnitude of 5.26 cm/sec. The majority of the spectral energy for both meters was at the semi-diurnal tidal frequency. The semi-diurnal tidal ellipse for 1028 had its major axis aligned in a northeast/southwest direction, and it encompassed north/south and east/west excursions comparable in magnitude to those of the deepwater meters 2918 and 2919. In addition to the diurnal and inertial peaks, 1028 also exhibited a significant spectral peak at about 6 hours, similar to the 6-hour peaks observed in the spectra for 2918 and 2919, which could be attributed to internal waves. Finally, the vector-averaged currents for 1028 were very similar to those of meter 2919, i.e., mostly northward, with an average vector magnitude of 1.33 cm/sec.

6.3 Observations on the Local Current Field

The general direction of flow for all seven current meter records from the 1975 and 1977-1978 deployments was predominantly northward and slightly upslope, with the greatest vector-averaged speeds occurring in the deeper water to the western part of the dumpsite area which encompasses both the 900 m and 1700 m dumpsites. The arithmetic mean speeds also show a decay in magnitude with proximity to the shore. Consequently, long term drift currents appear to dwindle in magnitude as one proceeds shoreward up the continental slope.

Semi-diurnal tidal energy also diminishes from the deeper western locations toward the eastern, shoreward locations. The tidal ellipses decrease in perimeter and change somewhat in orientation, from east/west in the deeper water to northeast/southwest toward shore. The greatest periodic energy components are observed along the east/west axes in the deeper water, and these magnitudes appear to diminish rapidly upslope. The orientation of the midwater ellipses, located partway upslope of the westernmost meters, is northwest/southeast, suggesting that midwater energies are directed more parallel than perpendicular to the shore.

6.4 Potential for Transport of Suspended Materials

On the basis of current speeds recorded during the two month period and in considering the sediment properties present at the waste disposal site, it may be concluded that resuspension of local sediments by bottom currents is unlikely. Sediment transport experiments and direct observations of sediment resuspension confirm the theory that fine-grained sediment requires relatively high (greater than 40 cm/sec) current speeds to place particles in motion (see Reference 4 for discussion; also Reference 9). This so-called "threshold velocity" and the factors influencing it are discussed in greater detail in a companion report (Reference 4, in press) detailing the results of a 1977 survey in this dumpsite area. Drift vectors obtained from the present study suggest that current magnitude decreases toward shore and this aspect, plus the diminished energies observed in shallower water, tend to reduce the net shoreward motion.

Due to the limited period during which the current meters were operational, it is clear that the nature of water motion at the waste disposal site requires further study which would include seasonal variables. Additional measurements further inshore would be of particular value as there is a seasonal current regime (the Davidson Current) which affects local circulation patterns.

SECTION 7

REFERENCES

1. Dayal, R., I.W. Duedall, M. Fuhrmann, and M.G. Heaton. 1979. Sediment and Water Column Properties at the Farallon Islands Radioactive Waste Dumpsites. Final report to the Office of Radiation Programs. U.S. Environmental Protection Agency, Washington, D.C.

2. Dyer, R.S. 1976. Environmental Surveys of Two Deep Sea Radioactive Waste Disposal Sites Using Submersibles. Proceedings of an International Symposium on Management of Radioactive Wastes from the Nuclear Fuel Cycle, Vol. 2. International Atomic Energy Agency, Vienna, Austria. IAEA-SM-207/65, p. 317-338.

3. Interstate Electronics Corporation. 1975. Operations Report: A Survey of the Farallon Islands 500-Fathom Radioactive Waste Disposal Site. U.S. Environmental Protection Agency, Office of Radiation Programs Technical Note ORP-75-1, Washington, D.C.

4. Interstate Electronics Corporation. 1982. Farallon Islands Oceanographic Data Analysis. Vol. I and II. Final Report to the Office of Radiation Programs, U.S. Environmental Protection Agency, Washington, D.C.

5. NOAA, Office of Coastal Zone Management. 1980. Draft Environmental Impact Statement on the Proposed Point Reyes-Farallon Islands Marine Sanctuary, p. E4-E9.

6. Noshkin, V.E., K.M. Wong, T.A. Jokela, R.J. Eagle, and J.L. Brunk. 1978. Radionuclides in the marine environment near the Farallon Islands. Lawrence Livermore Laboratory, University of California Report No. UCRL-52381, Livermore, California.

7. Schwartzlose, R. Scripps Institution of Oceanography. La Jolla, California. Unpublished materials received December 1980 and August 1982, including raw data records for meters 1009 and 1028, and subsequent analysis.

8. Wilde, P. 1976. Oceanographic data off central California, 37° to 40° north including the Delgada deep sea fan. Lawrence Berkeley Laboratory Pub. No. 92, University of California, Berkeley, California.

9. Larsen, L.H., R. W. Sternberg, N.C. Shi, M.A.H. Marsden, and L. Thomas. 1981. Field investigations of the threshold of grain motion by ocean waves and currents. In Sedimentary Dynamics of Continental Shelves. Elsevier, Amsterdam, reprinted as Developments in Sedimentology, Vol. 32, p. 105-132, C.A. Nittrouer, ed. 449 p.

TECHNICAL REPORT DATA
(Please read Instructions on the reverse before completing)

1. REPORT NO. EPA 520/1-83-019	2.	3. RECIPIENT'S ACCESSION NO.
4. TITLE AND SUBTITLE Analysis of Ocean Current Meter Records Obtained from a 1975 Deployment Off the Farallon Islands, California		5. REPORT DATE August 1983
		6. PERFORMING ORGANIZATION CODE
7. AUTHOR(S) David E. Crabbs		8. PERFORMING ORGANIZATION REPORT NO.
9. PERFORMING ORGANIZATION NAME AND ADDRESS Interstate Electronics Corporation Anaheim, California 92803		10. PROGRAM ELEMENT NO.
		11. CONTRACT/GRANT NO. IAG No. AD-89-F-1-607-0 Subcontract No. B-C2076-A-X
12. SPONSORING AGENCY NAME AND ADDRESS Office of Radiation Programs U.S. Environmental Protection Agency 401 M Street., S.W. Washington, D.C. 20460		13. TYPE OF REPORT AND PERIOD COVERED Final
		14. SPONSORING AGENCY CODE ANR-461

15. SUPPLEMENTARY NOTES

16. ABSTRACT

Two bottom current records were obtained during August and September 1975 in the Farallon Islands low-level radioactive waste disposal area off San Francisco, California. This report presents the results of the data reduction and analysis of the curent meter records,and interprets the results with respect to additional data collected in 1977. An effort is made to compare the patterns of current activity in the dumpsite area for the time periods measured. It is proposed that while the possibility of transport of suspended material from within the dumpsite area cannot be ignored, conditions which prevailed at the time and location of measurements suggest that there is little tendency for shoreward transport of resuspended sediment. However, measurements taken throughout the year and over a wider area would be helpful in verifying this propositon.

17. KEY WORDS AND DOCUMENT ANALYSIS

a. DESCRIPTORS	b. IDENTIFIERS/OPEN ENDED TERMS	c. COSATI Field/Group
Ocean Dumping Ocean Disposal/Sea Disposal Low-Level Radioactive Waste Disposal Ocean Bottom Currents off California Radioactivity Transport		

18. DISTRIBUTION STATEMENT Unlimited Release	19. SECURITY CLASS *(This Report)* Unclassified	21. NO. OF PAGES
	20. SECURITY CLASS *(This page)* Unclassified	22. PRICE

EPA Form 2220-1 (Rev. 4-77) PREVIOUS EDITION IS OBSOLETE